



RESERVOIR CHARACTERIZATION PROJECT

Rock Physics Modeling of Tight Gas Sands Lajas – Neuquén Basin

Atilas Silva
Master's Student

Topics

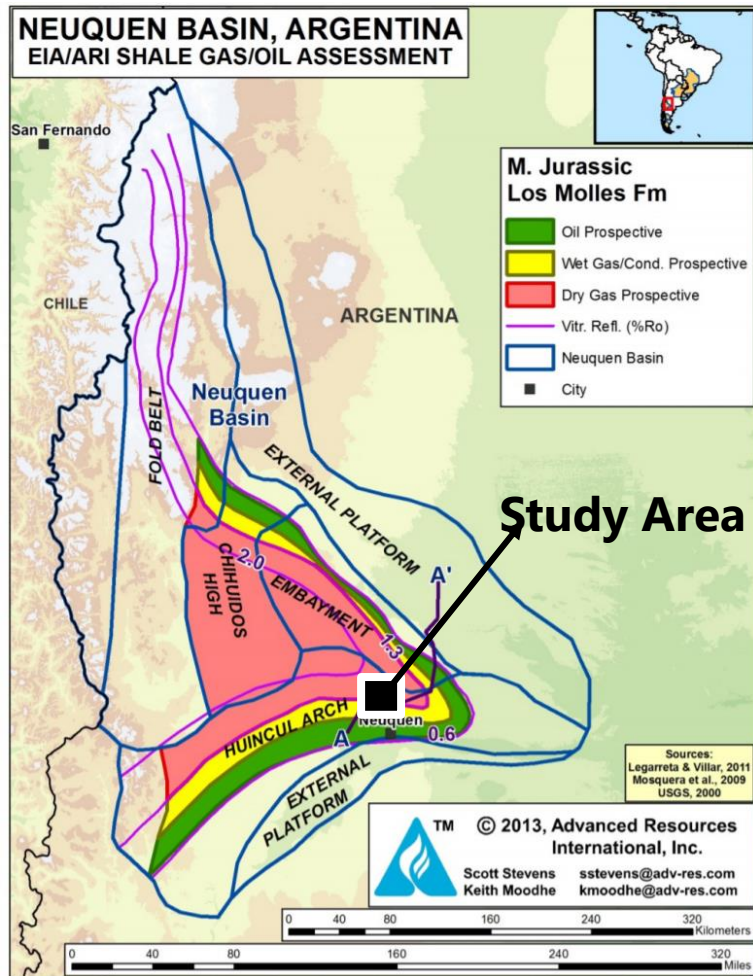
- 🔹 Objectives
- 🔹 Location and geologic setting
- 🔹 Data available
- 🔹 Rock physics modeling
- 🔹 Conclusions and future work

Research Objectives

- 💧 Develop a rock physics model that can best represent the seismic response of the tight sand of the study area
- 💧 Construct rock physics templates aiming to quantitatively predict the seismic response as a function of key rock properties (porosity, pore aspect ratio, gas saturation, fracture density, pore pressure, etc.)
- 💧 Identify sweet spots in the seismic inversion data

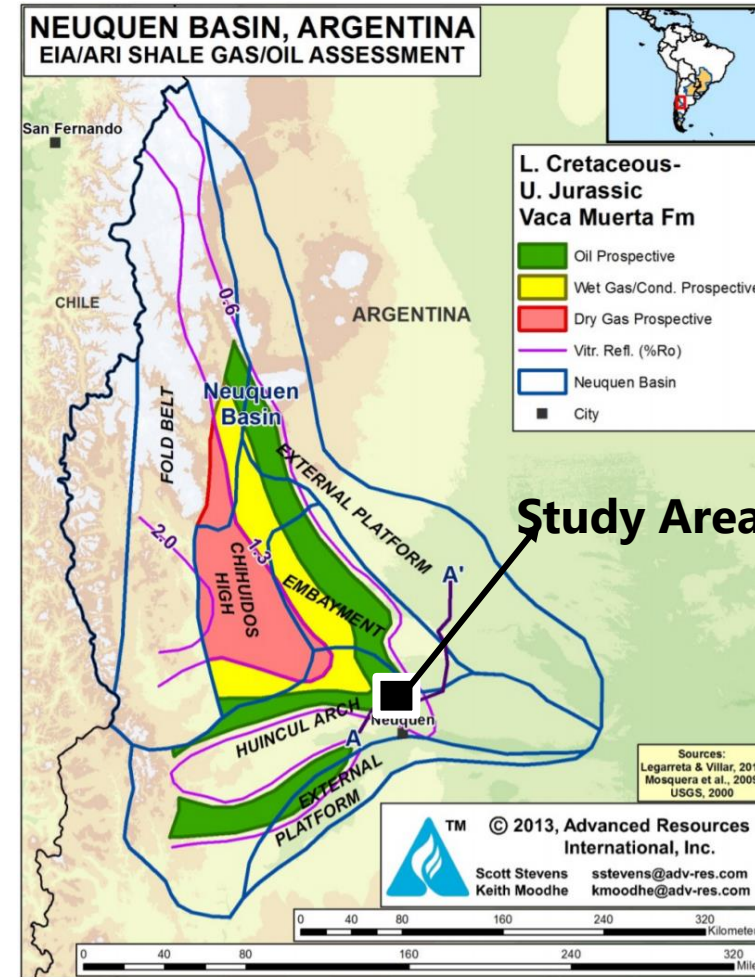
Thermal Maturity Map

Los Molles



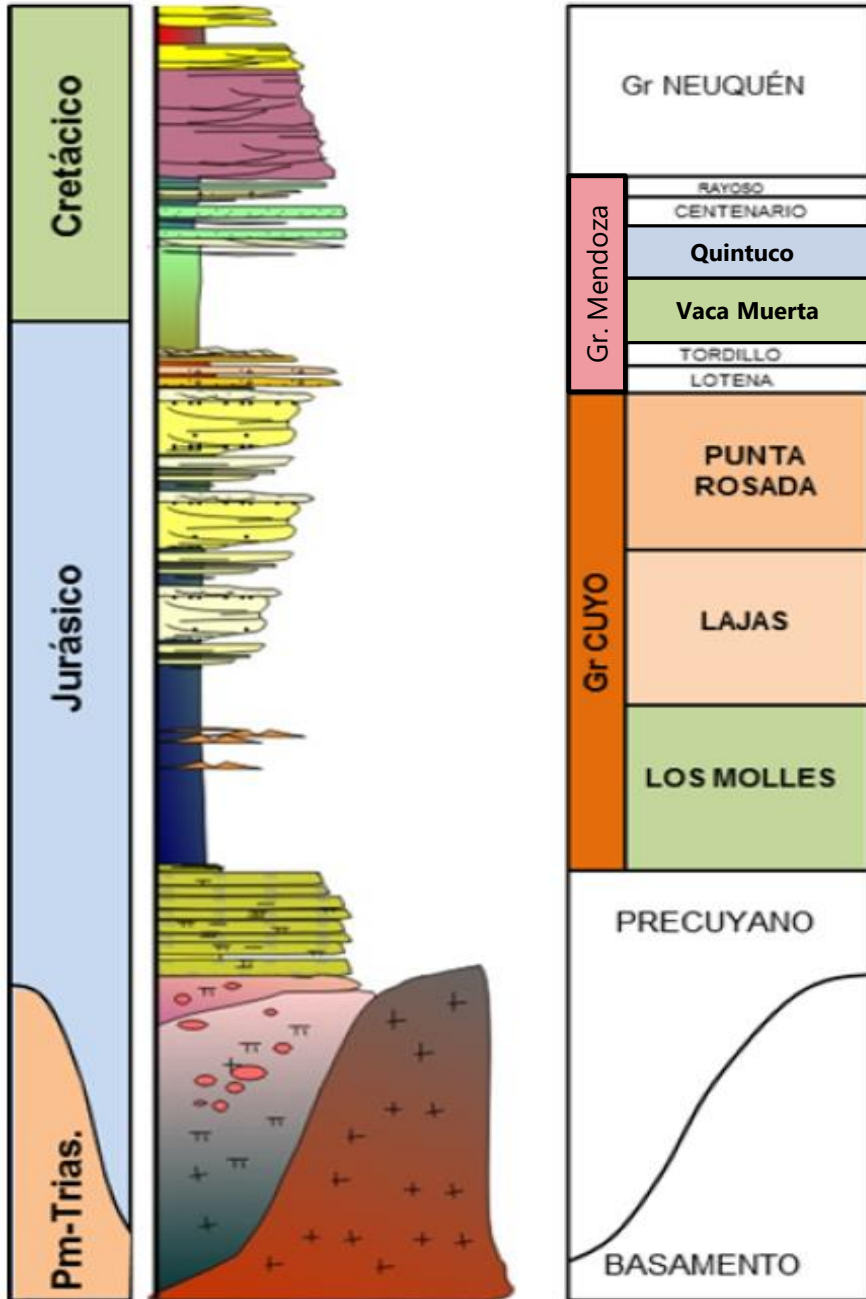
Source: ARI, 2013.

Vaca Muerta



Source: ARI, 2013.

Petroleum Systems in the area



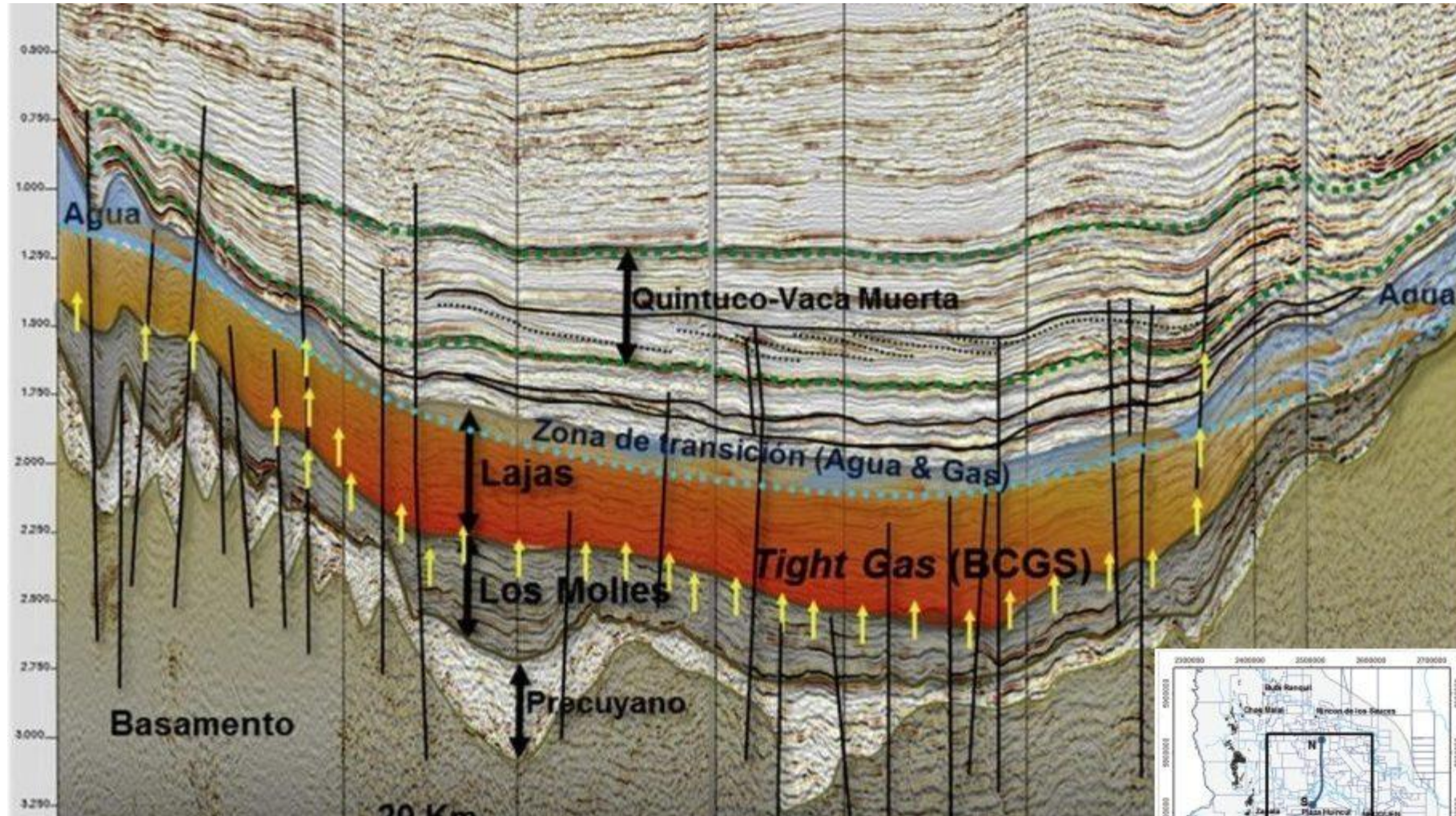
Conventional

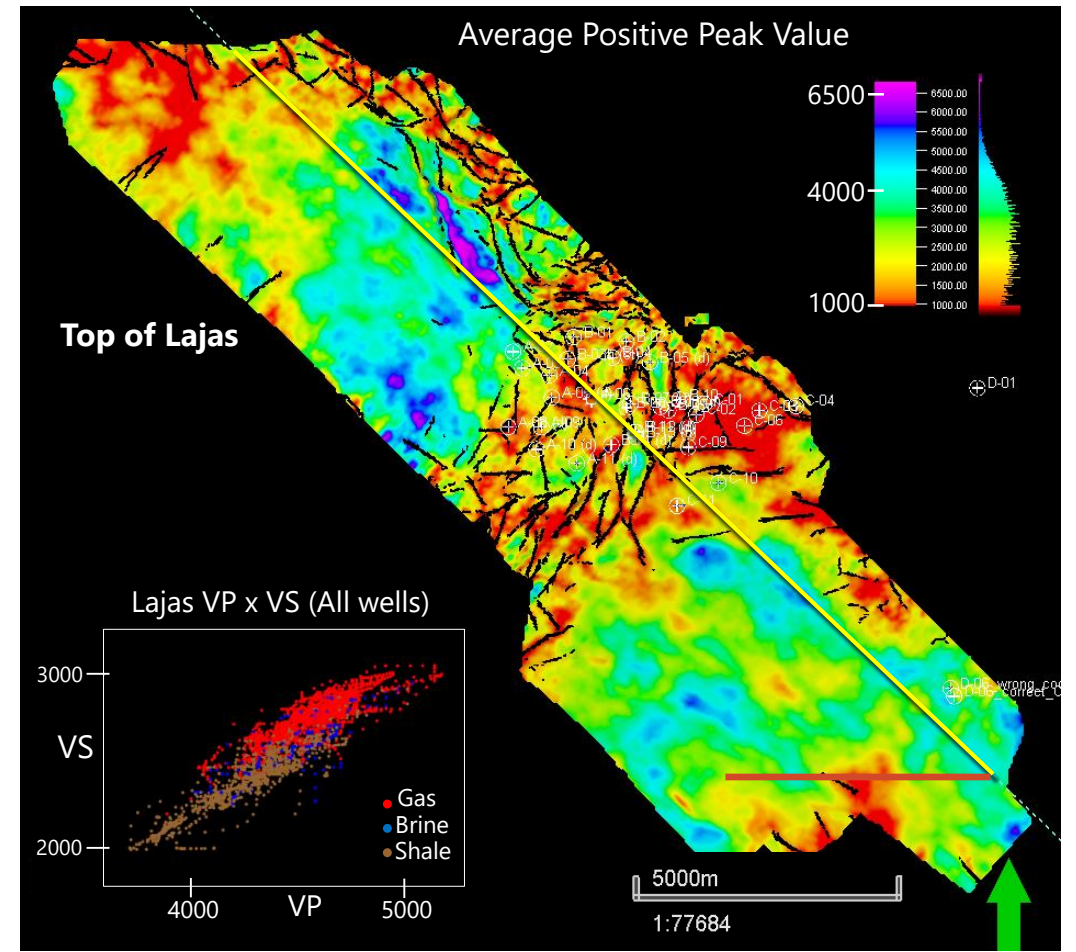
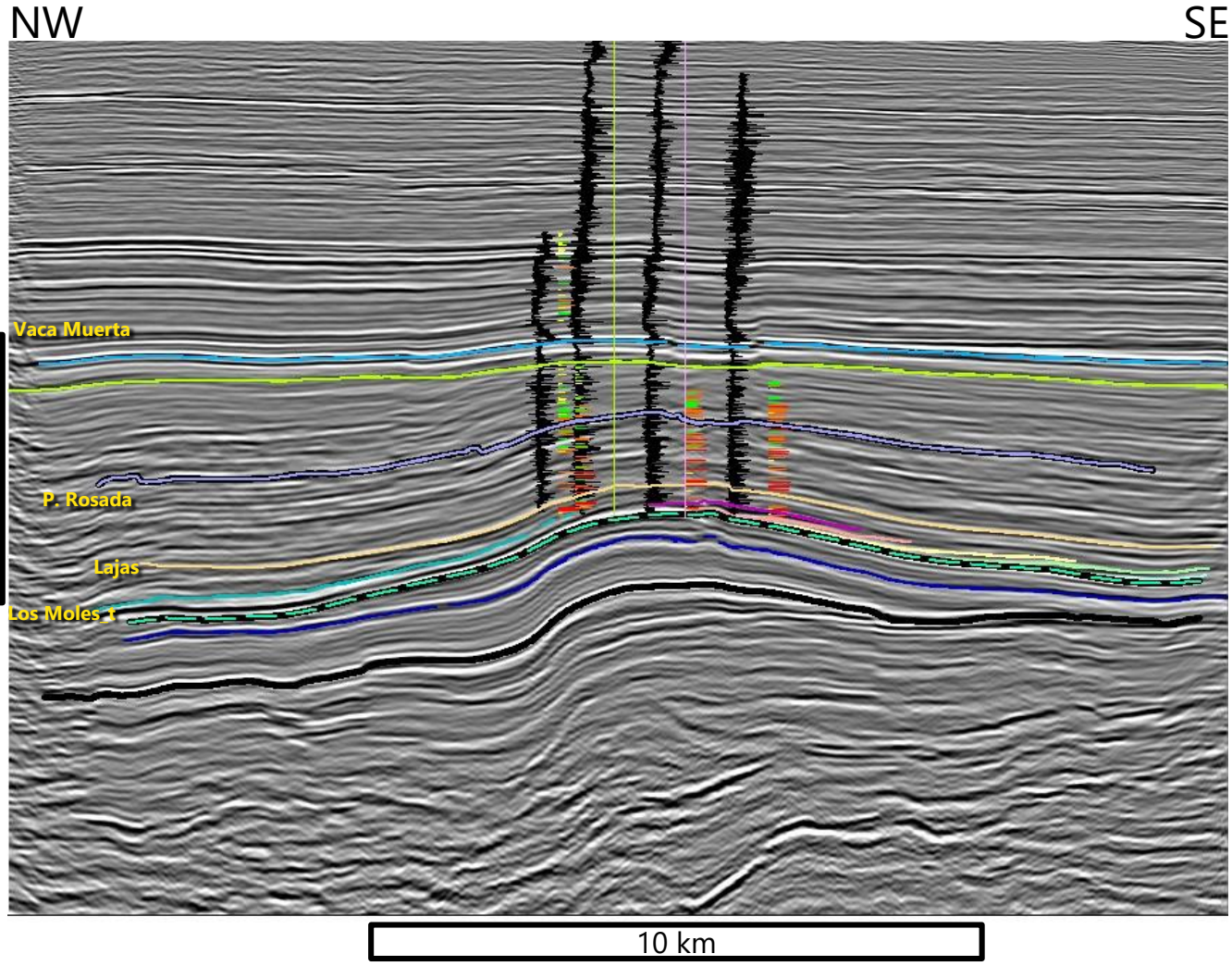
- Carbonates from the Quintuco Formation
- **Vaca Muerta** Source Rock

Unconventional

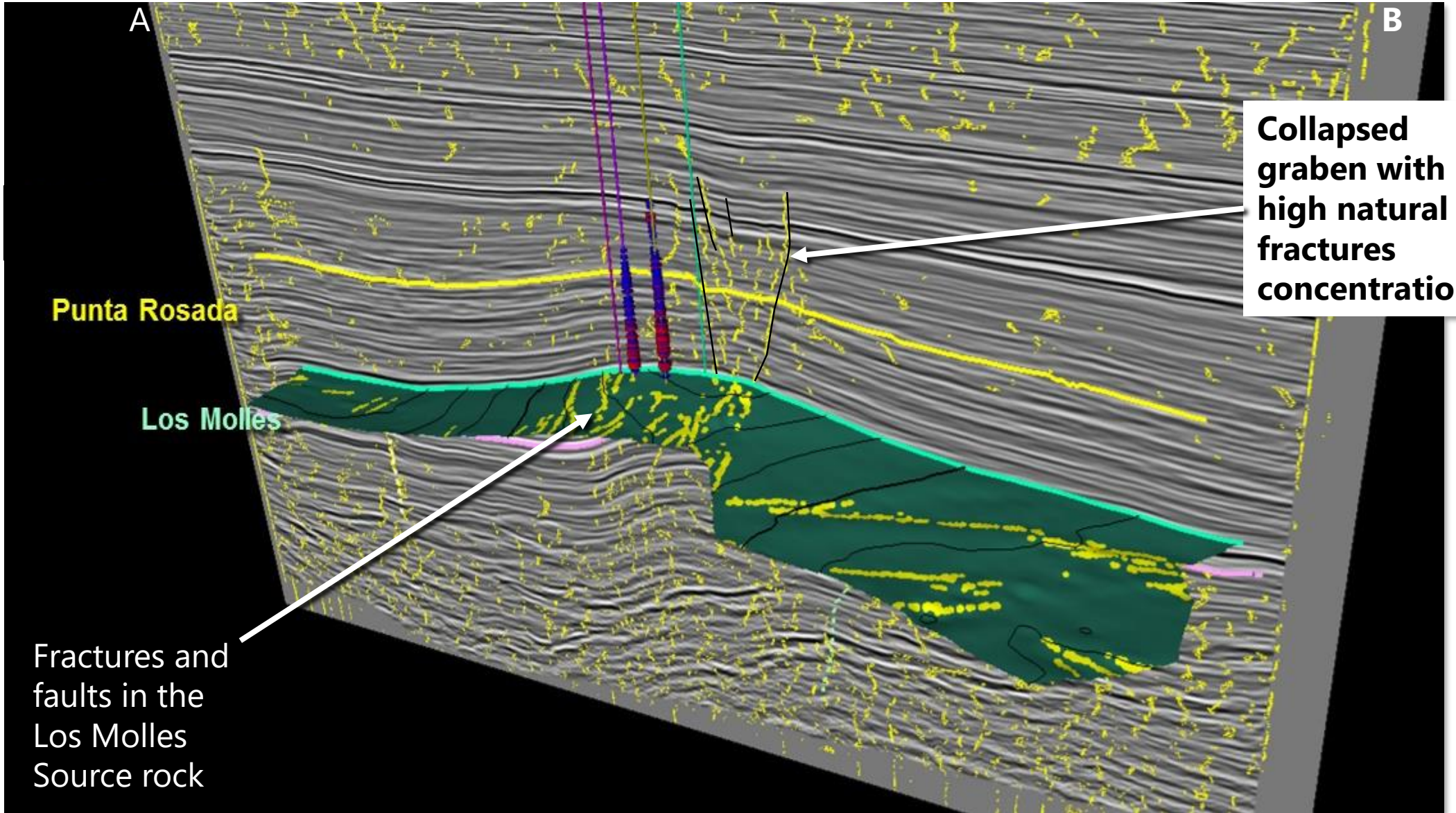
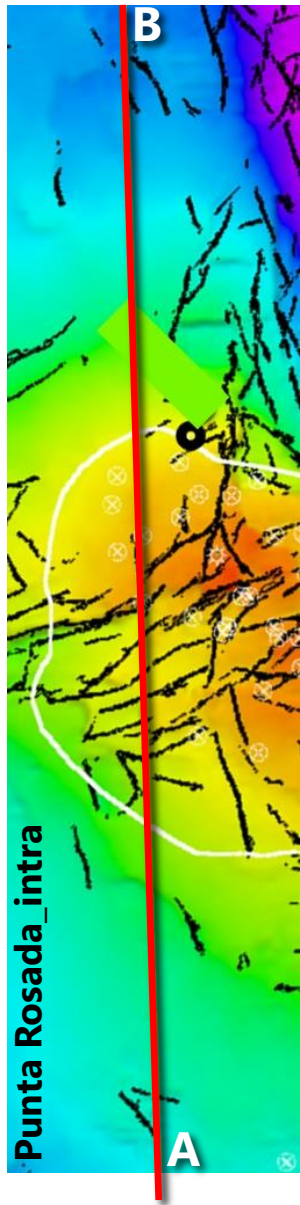
- Tight Sands
- **Lajas e Punta Rosada**
- Ranging from 900 to 1500m of thickness
- Porosity: 4 to 10%
- Permeability: < 0.1 mD
- **Los Molles** Source Rock

Overpressurized tight sands





Natural Fracture Network



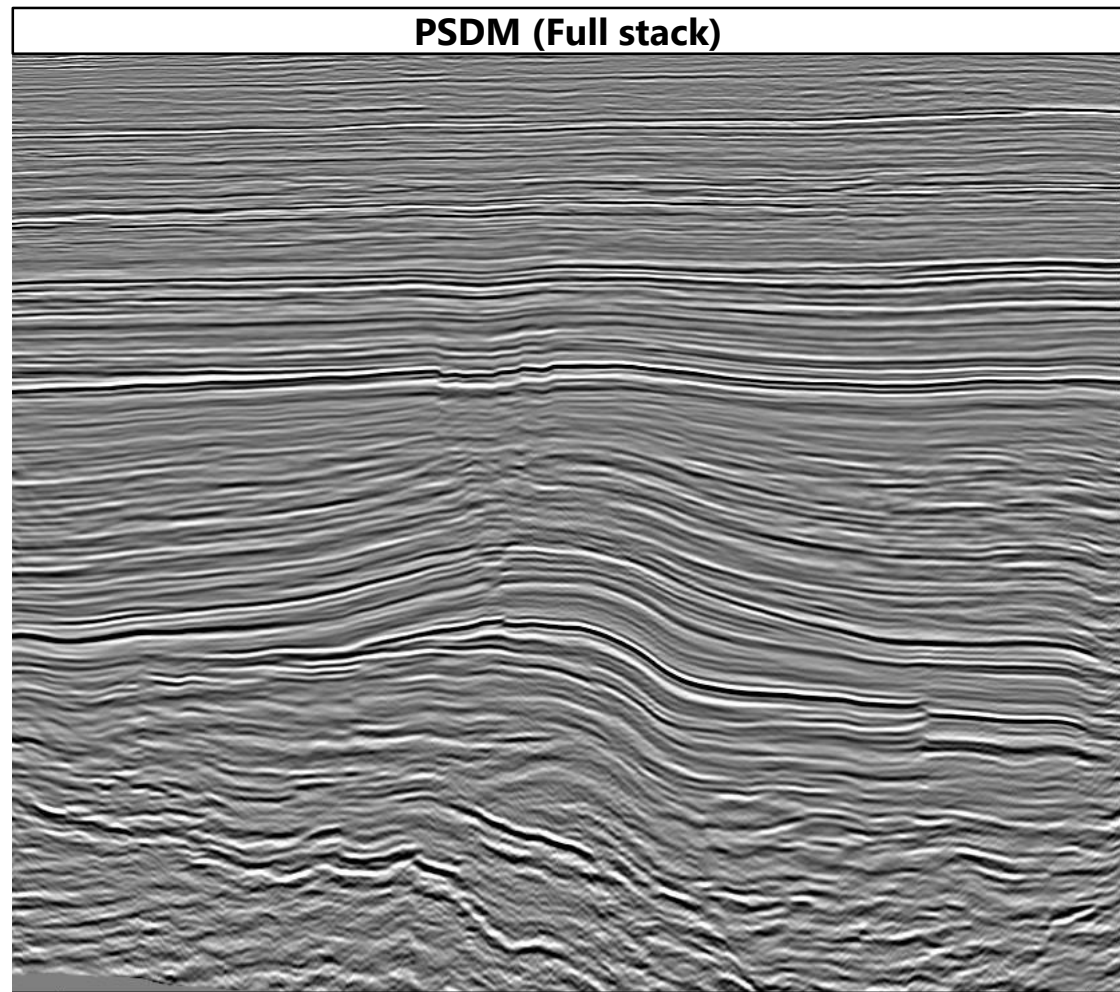
Data Available

Seismic

- PSDM and PSTM
- Full Stacks
- Angle Stacks (Problem in the Far Stack)

29 Wells

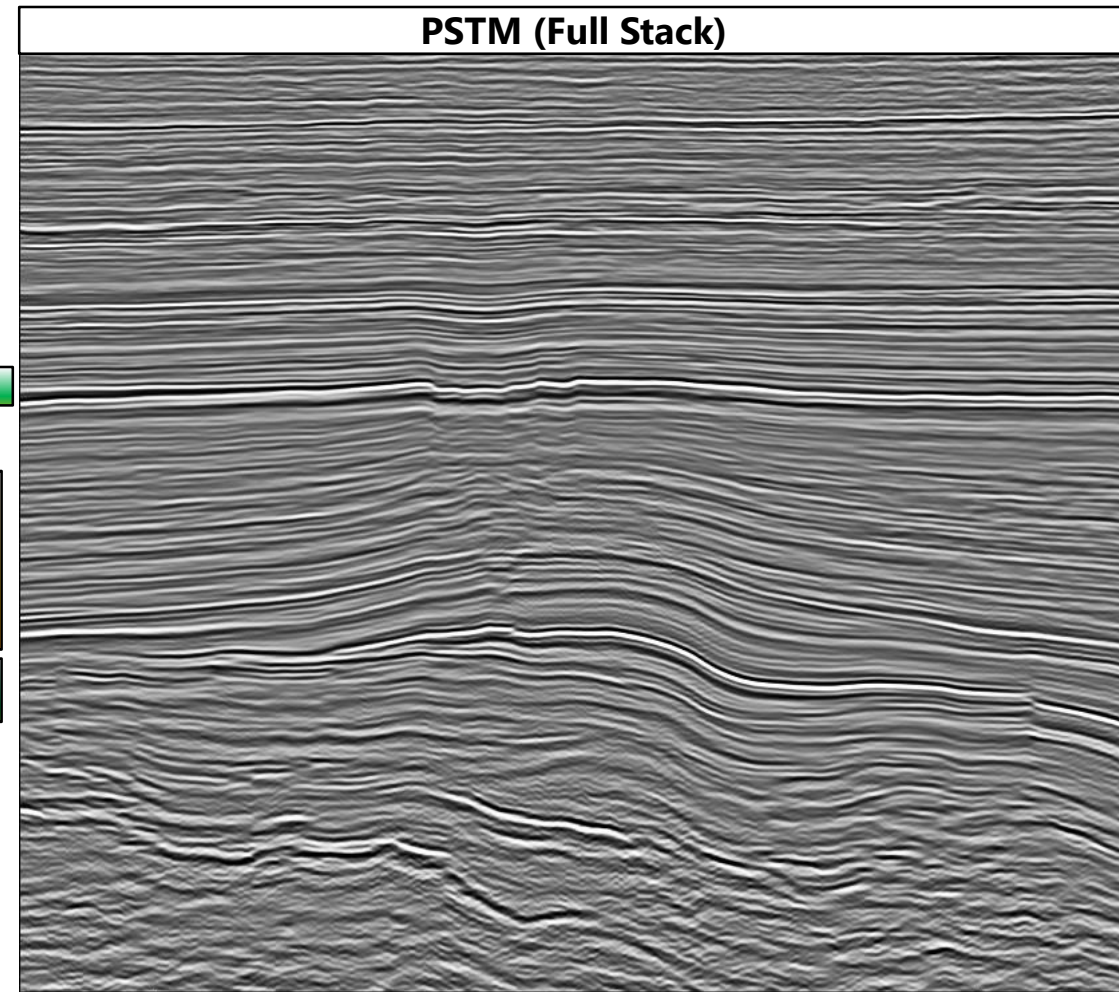
Processed in 2015



V. Muerta

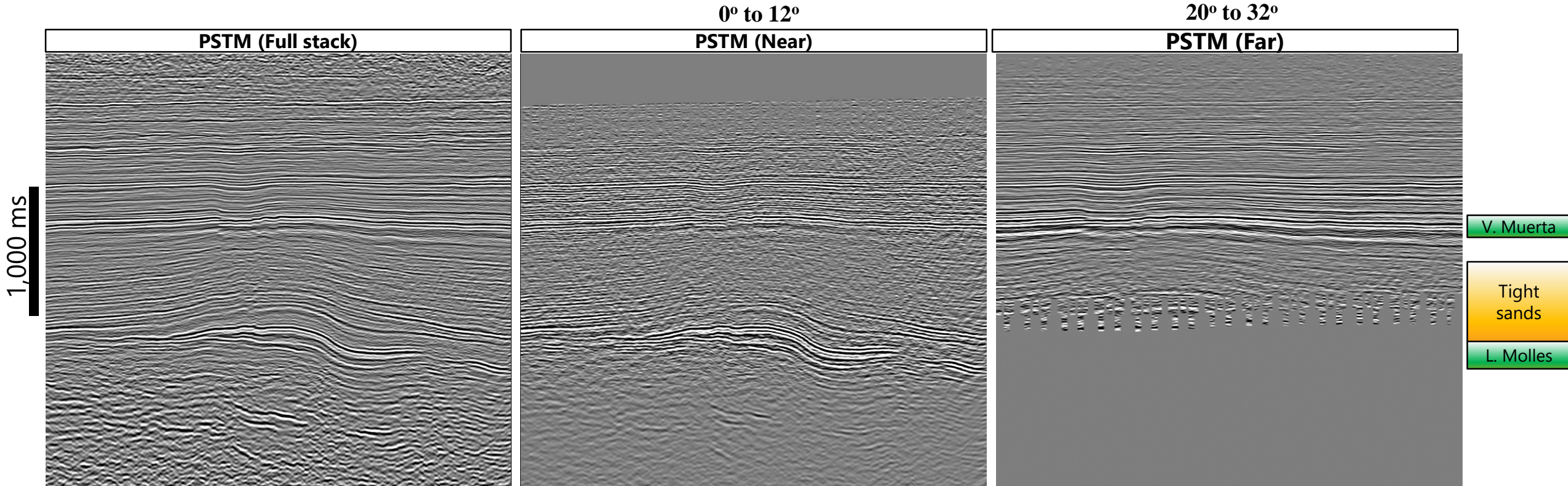
Tight
sands

L. Molles



Processed in 1998

10° to 22°
MID





ROCK PHYSICS MODELING

Lajas Formation

Seismic response for Sandstones

High porosity sandstone:

- Mineral composition
- Porosity
- Fluid type

Seismic response for Sandstones

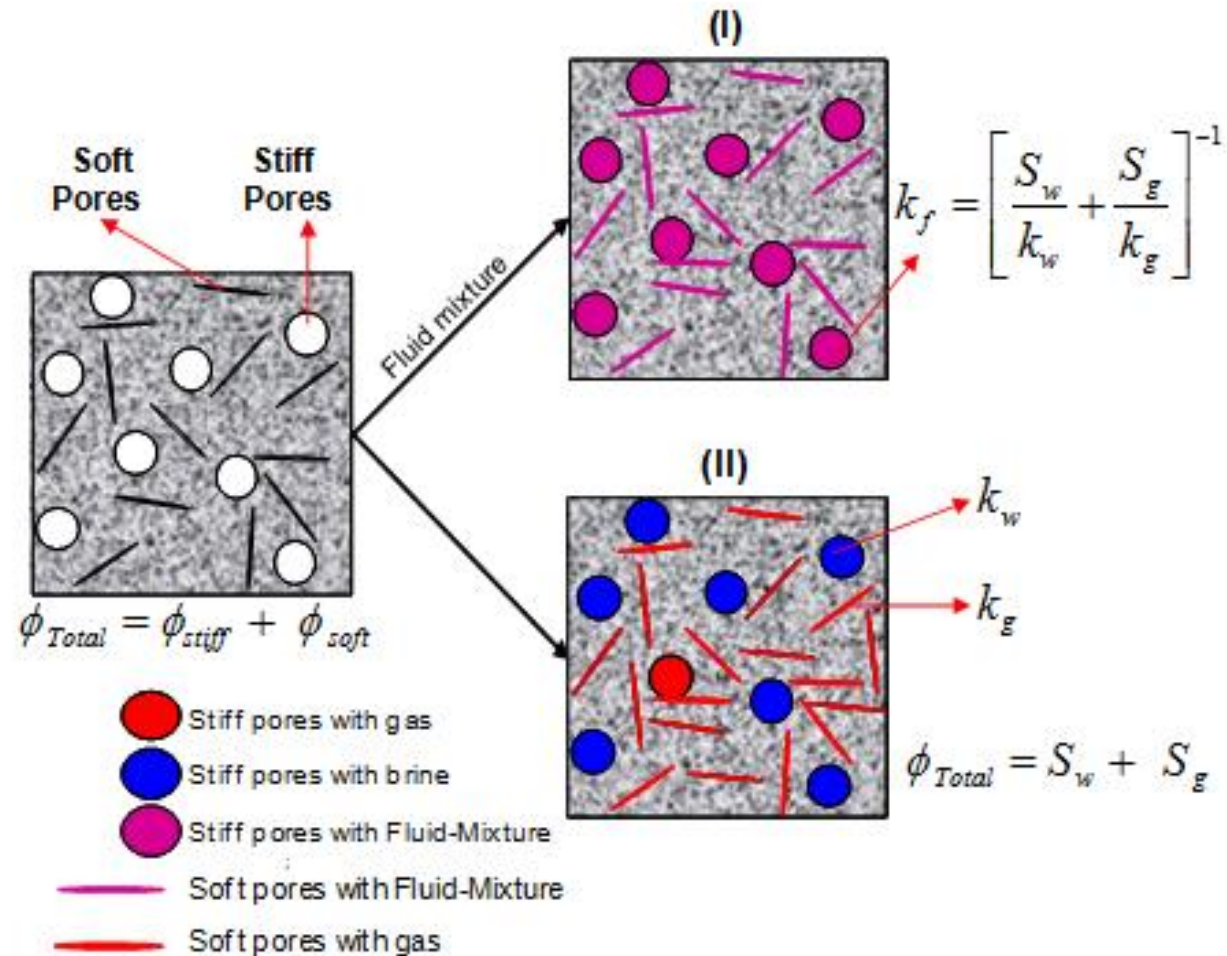
💧 High porosity sandstone:

- Mineral composition
- Porosity
- Fluid type

💧 Tight sandstone:

- Most influenced by **Pore structure**.
- An increase in velocity is mainly due to the closure of micro-cracks and compliant pores.

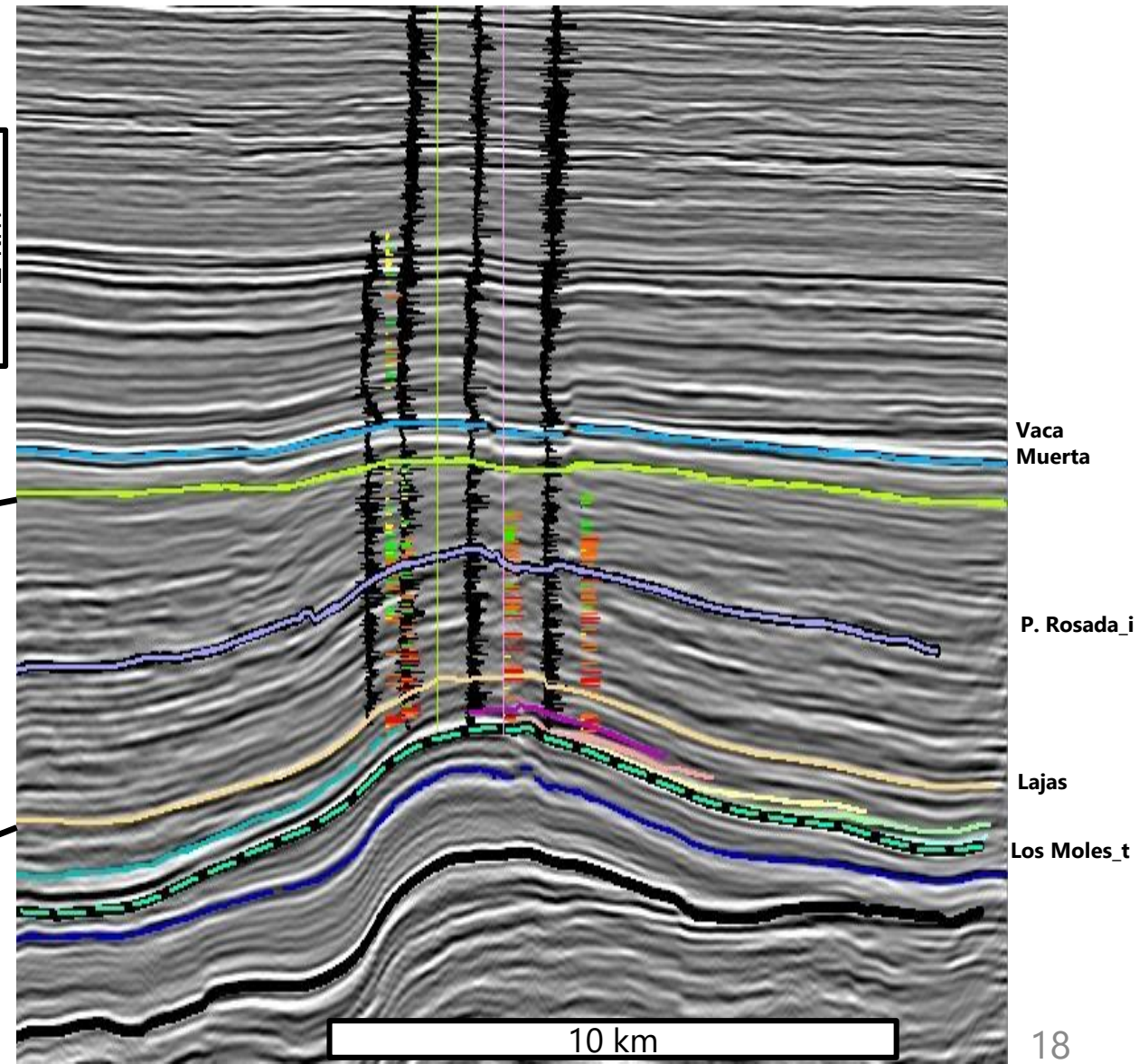
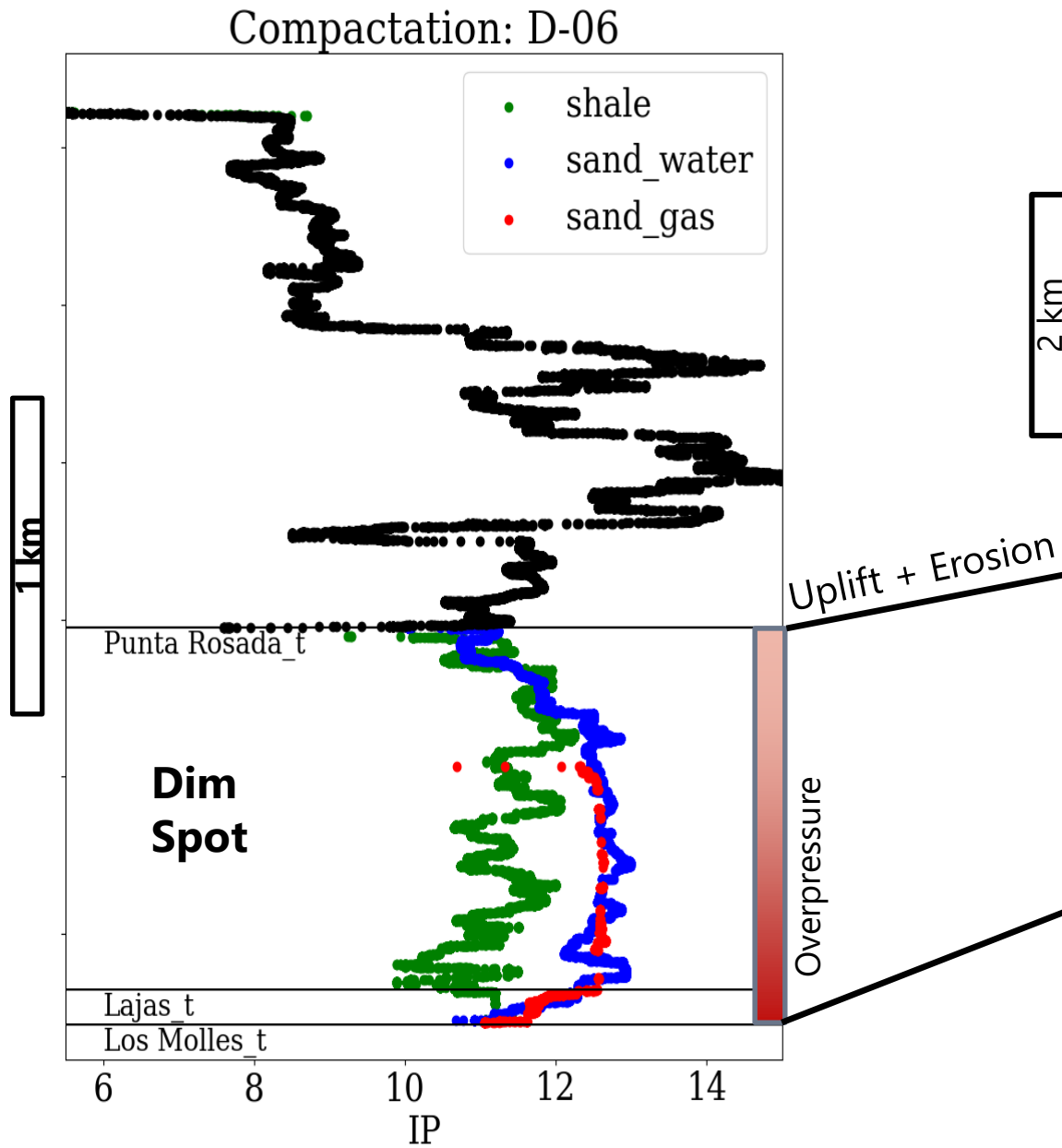
Inclusion-based Rock Physics Models



Effective medium approximations based on inclusions with different pore shapes can model the elastic moduli of low porosity rocks

Reservoir Characteristics

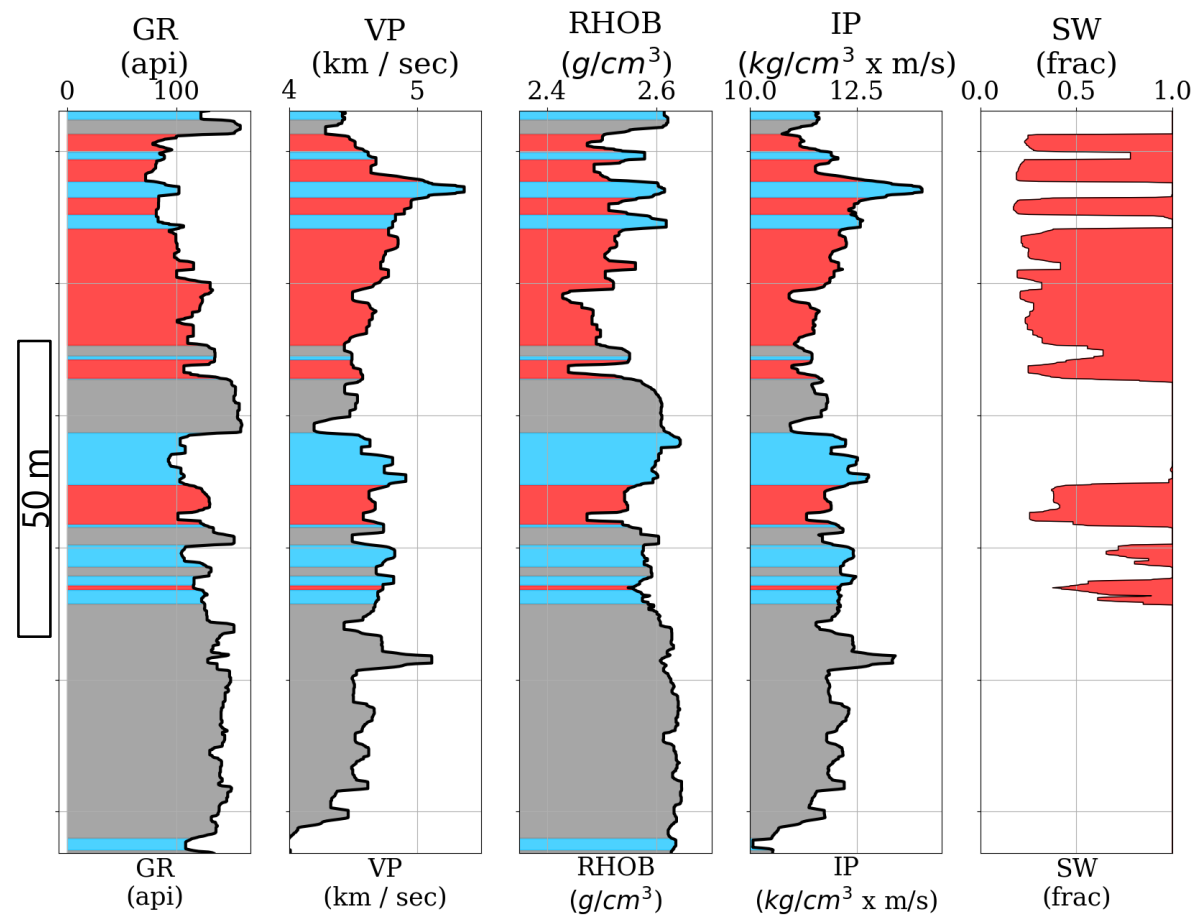
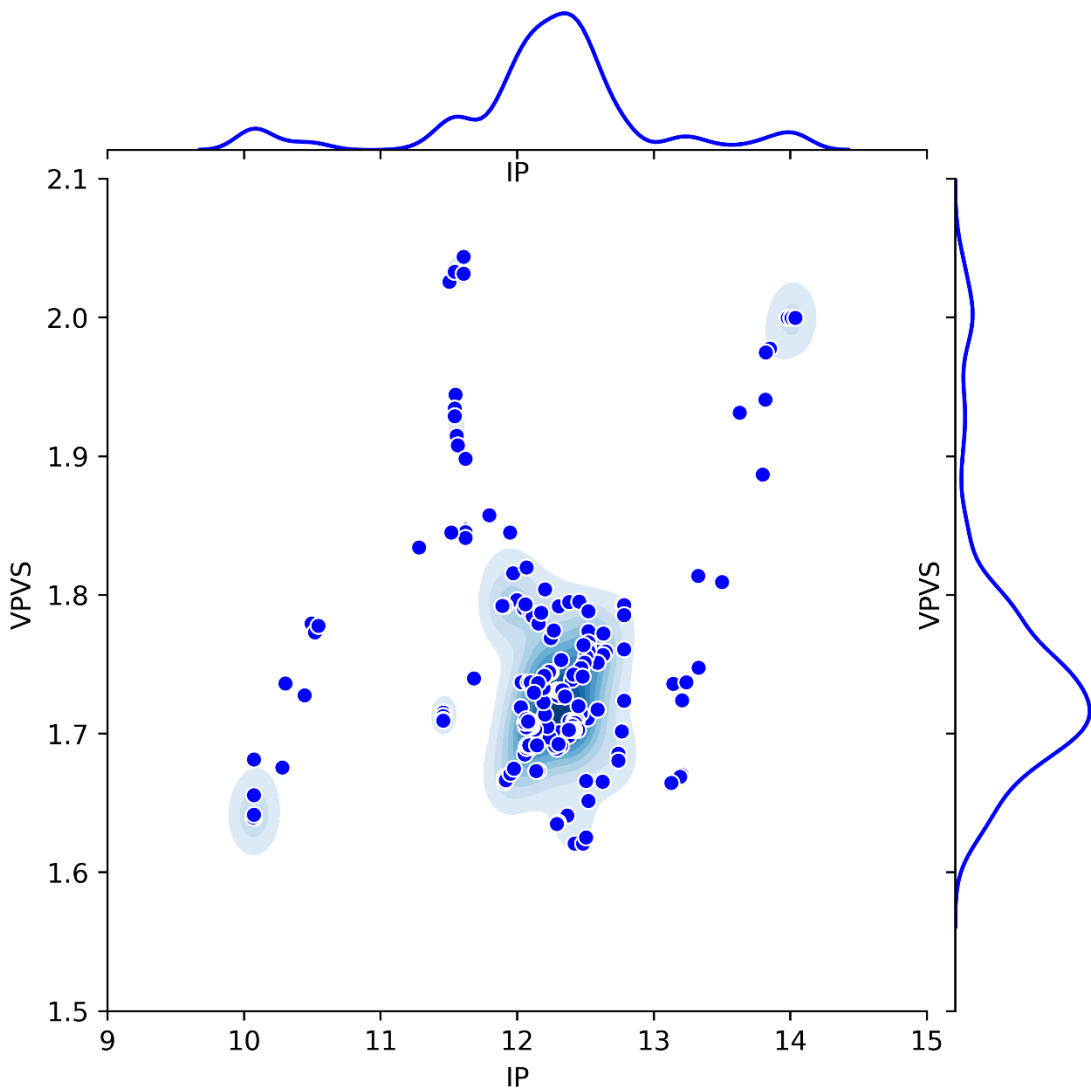
Compaction



Well A-10

Reservoir Cut-offs

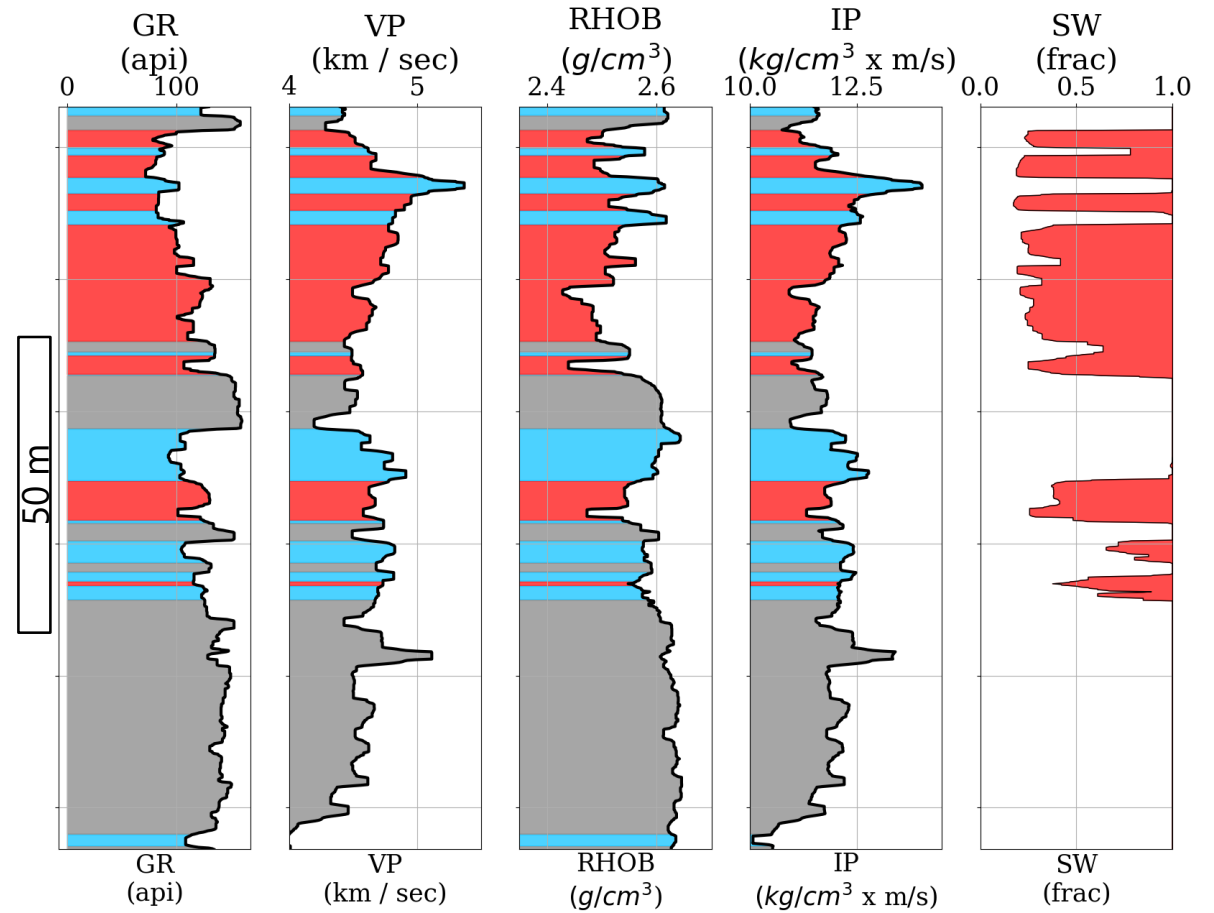
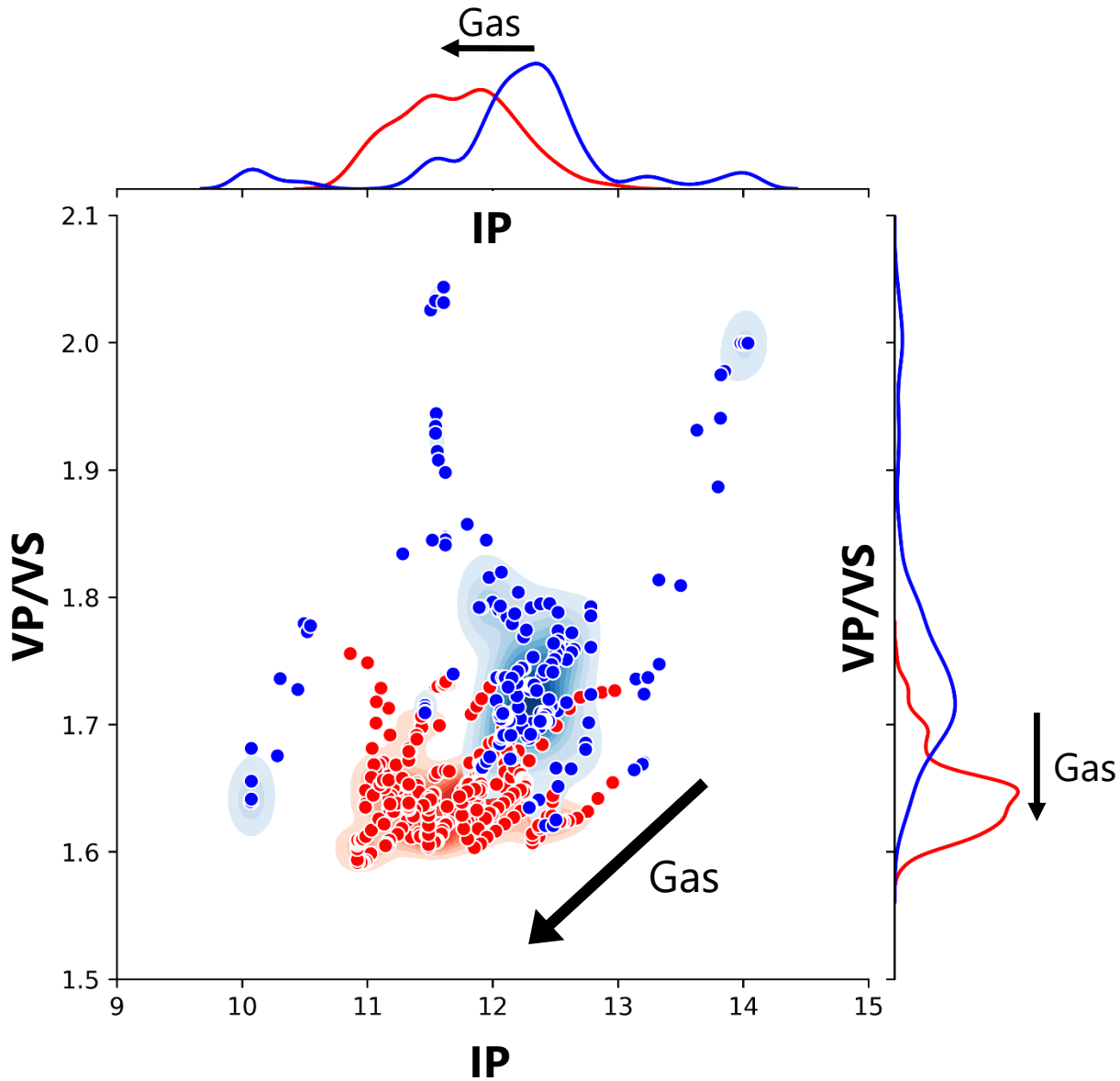
| | Gas | Brine | Shale |
|------|-------|-------|-------|
| Clay | < 20% | | > 20% |
| PHIe | > 4% | | -- |
| Sw | < 50% | > 50% | -- |



Well A-10

Reservoir Cut-offs

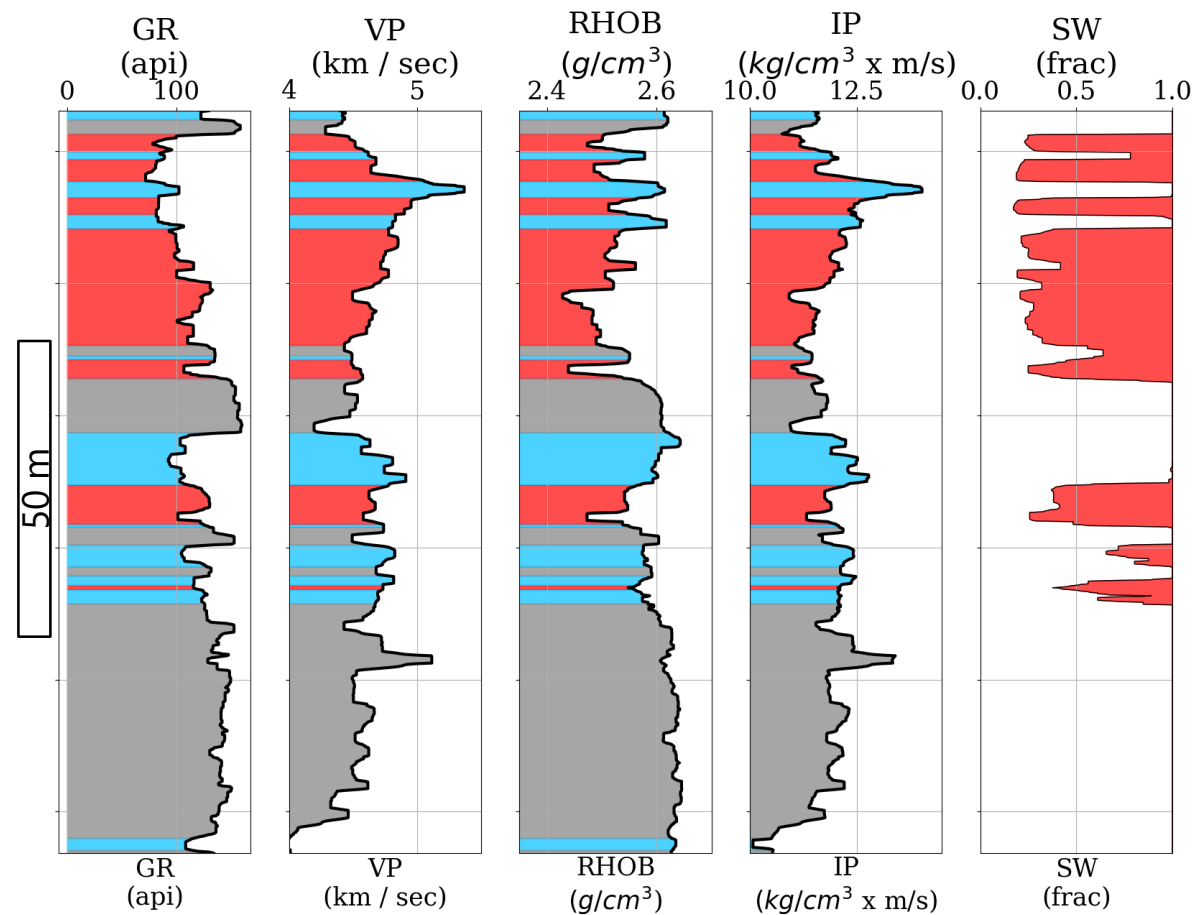
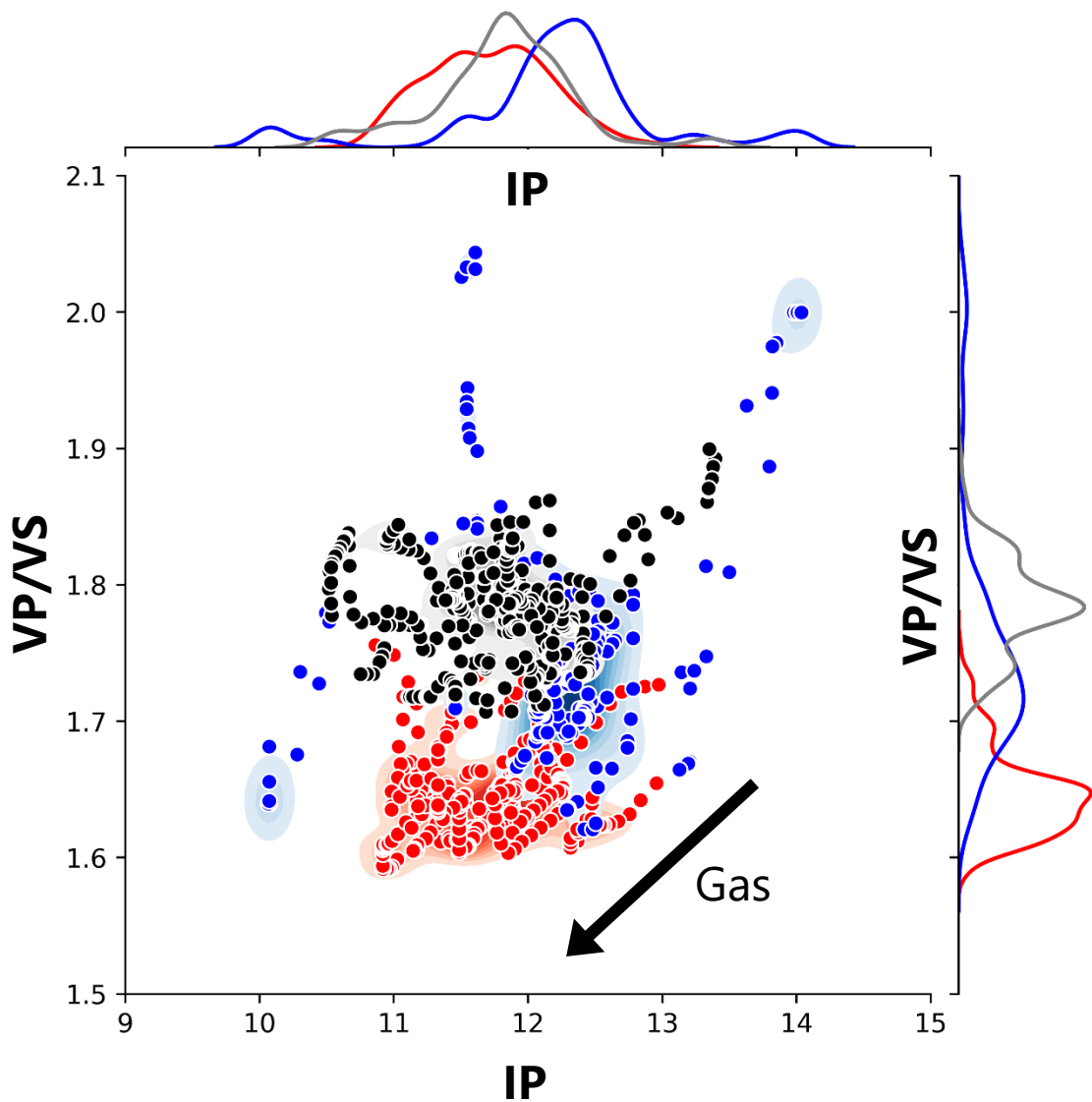
| | Gas | Brine | Shale |
|------|-------|-------|-------|
| Clay | < 20% | | > 20% |
| PHIe | > 4% | | -- |
| Sw | < 50% | > 50% | -- |



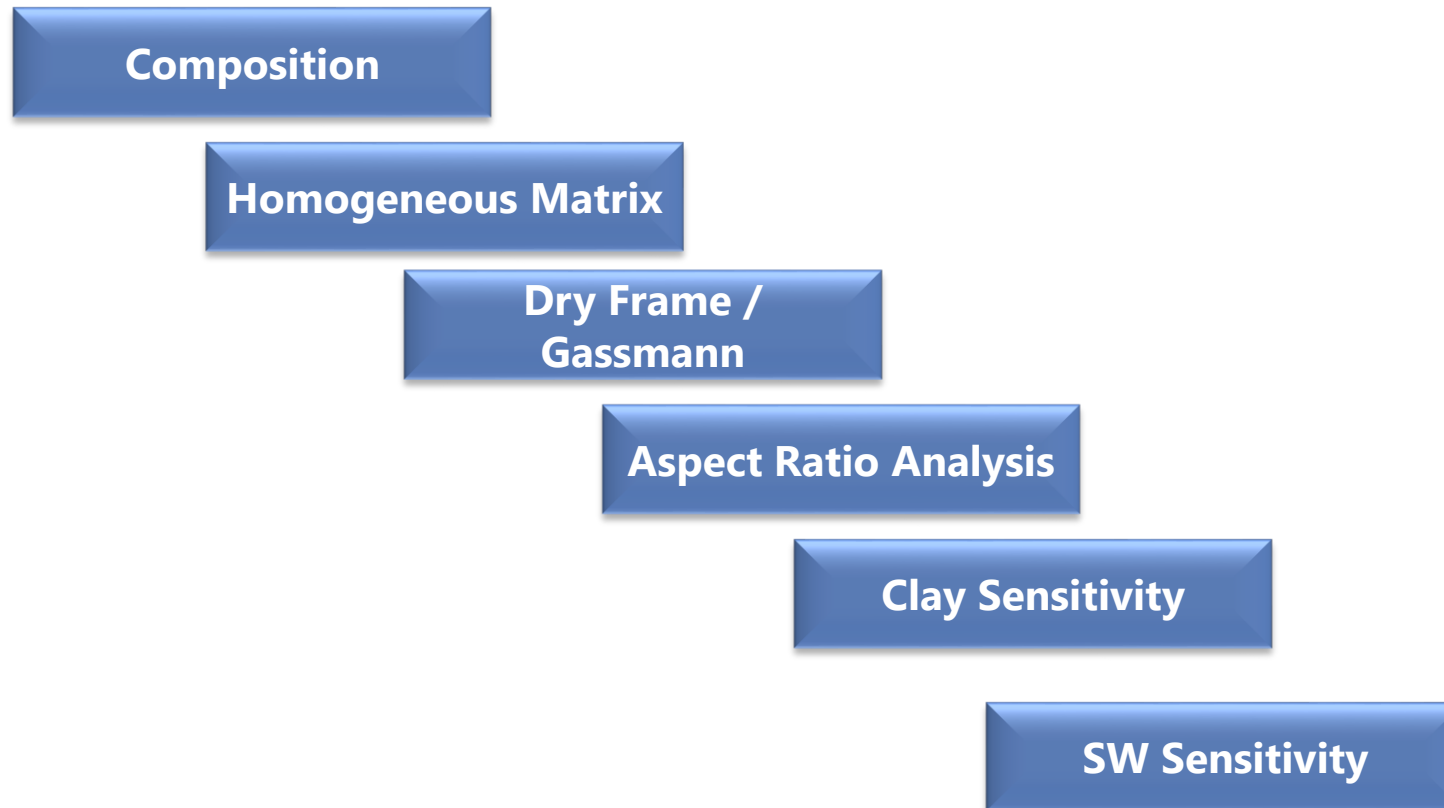
Well A-10

Reservoir Cut-offs

| | Gas | Brine | Shale |
|------|-------|-------|-------|
| Clay | < 20% | | > 20% |
| PHIe | > 4% | | -- |
| Sw | < 50% | > 50% | -- |



Rock Physics Model



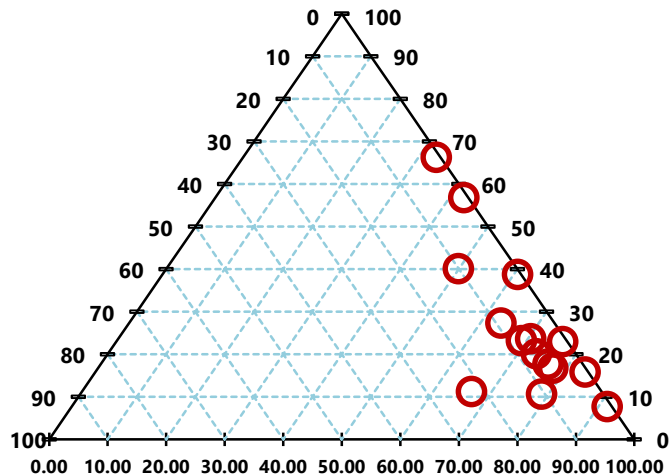
Reservoir Composition

X-Ray Diffraction – 6 Wells

Chlorite

5.8 %

(k = 95 GPa)



Kaolinite

26.5 %

K = 1.5 Gpa

Illite

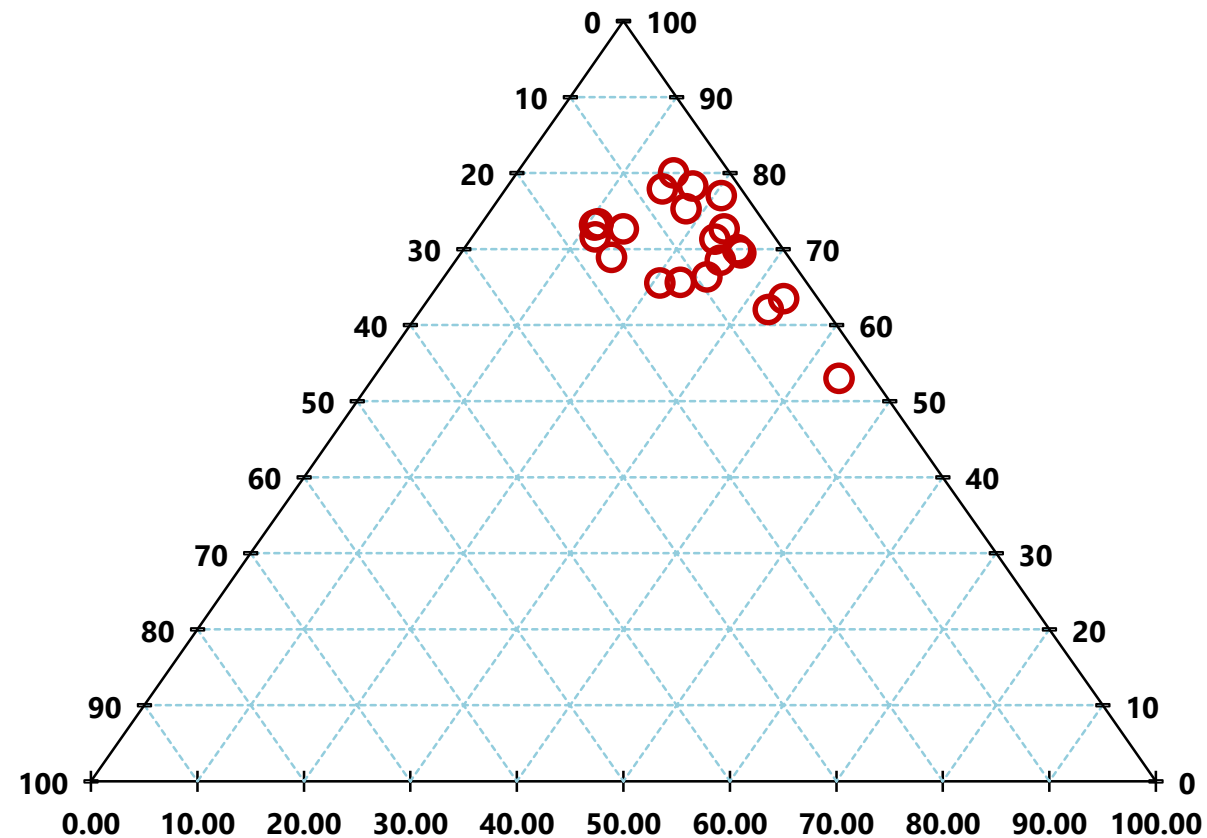
67.6 %

K = 39 Gpa

Quartz

70.3 %

K = 37 Gpa



Clay

8.4 %

K = Large range

Feldspars

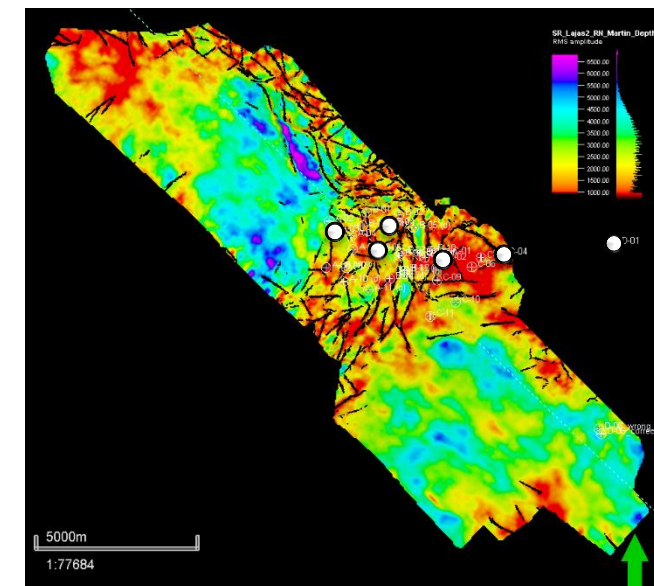
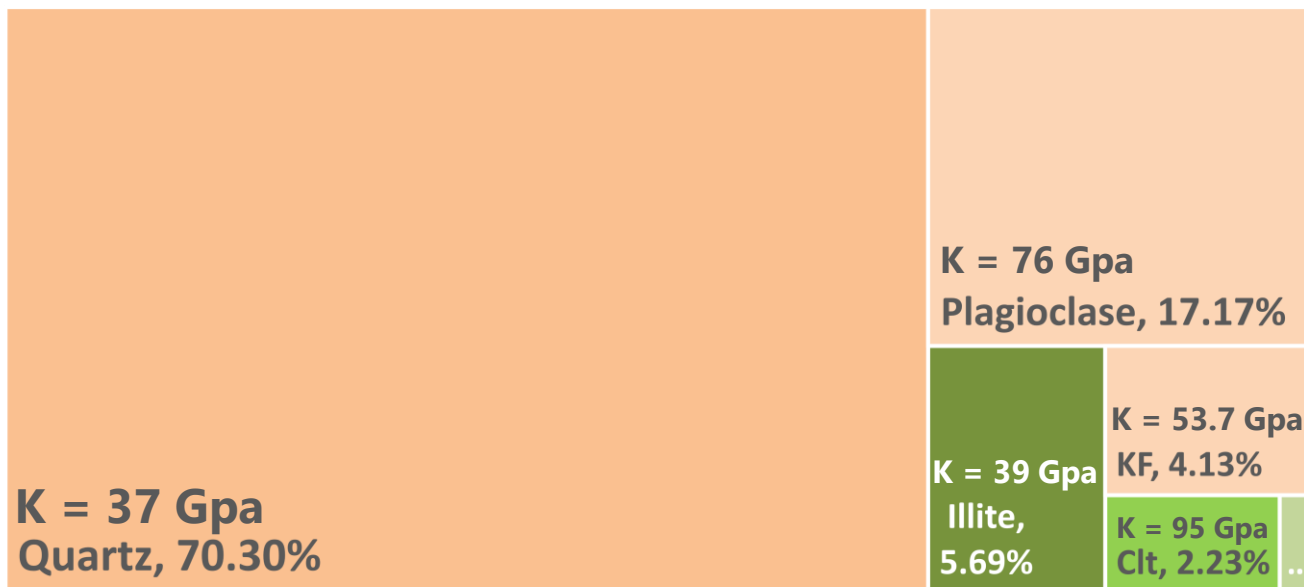
21.3 %

K = 60 Gpa

Reservoir Composition

X-Ray Diffraction – 6 Wells

■ Clt ■ Illite ■ Caolinite ■ Quartz ■ Plagioclase ■ KF



Silicate Background (91.6%)

QTZ + PLG + KF

$K = 44.2 \text{ Gpa}$
 $\mu = 39 \text{ GPa}$
 $\rho = 2.64 \text{ g/cm}^3$

Homogeneous Clay (8.4%)

Illite + Clt + kaolinite

$K = 51 \text{ Gpa}$
 $\mu = 12 \text{ GPa}$
 $\rho = 2.80 \text{ g/cm}^3$

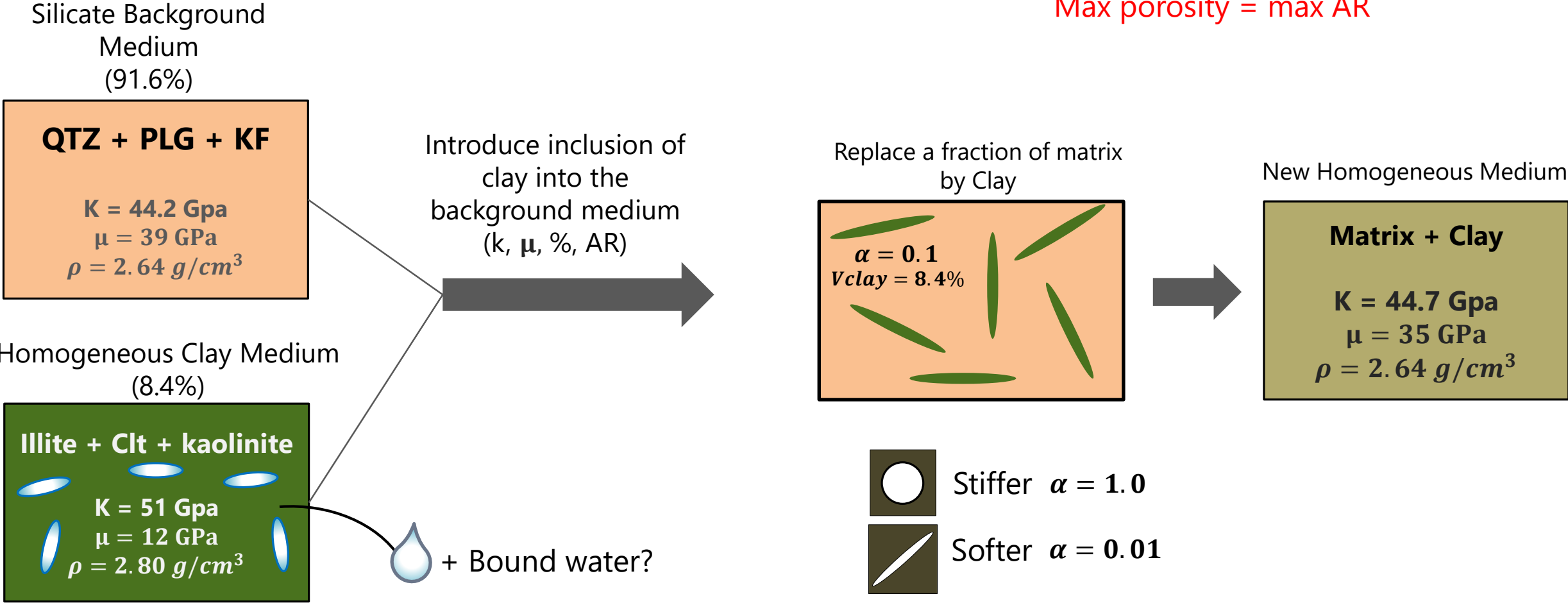
Two Homogeneous medium

(Voigt-Reuss-Hill)

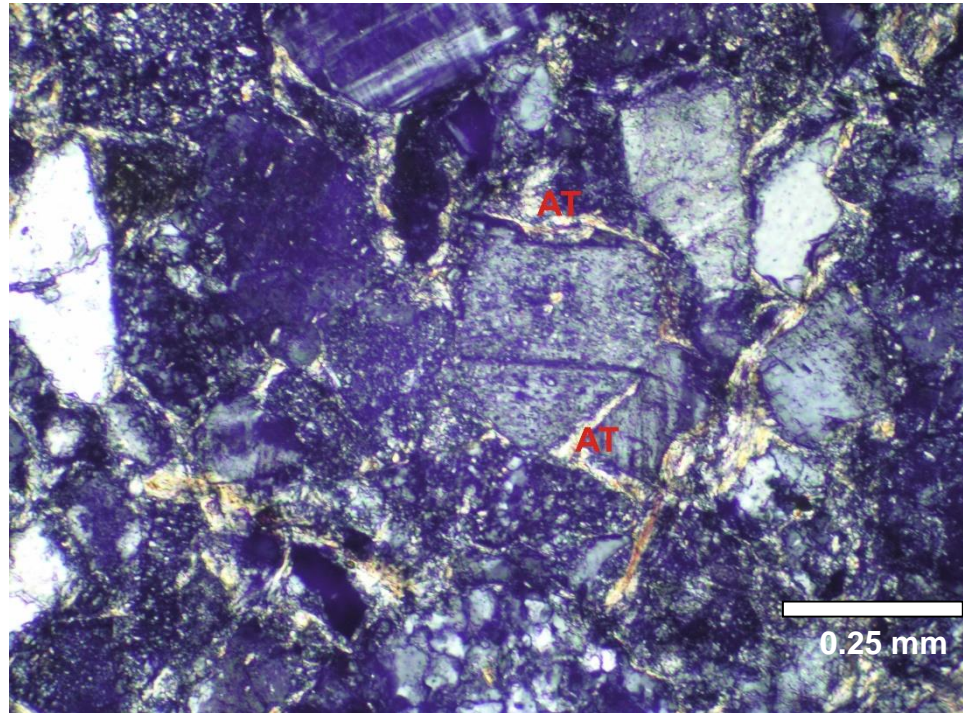
Kuster–Toksöz, 1974

Adding inclusions of clay into silicate background medium

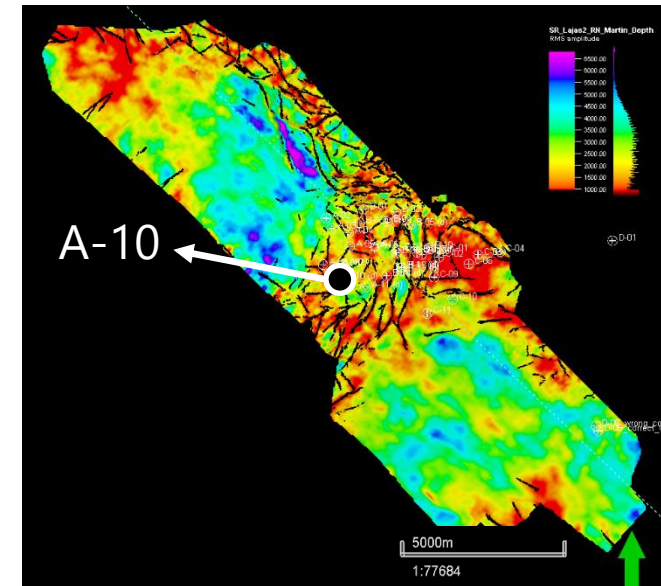
Max porosity = max AR



Clay



A-10: Early inter-grain clay.

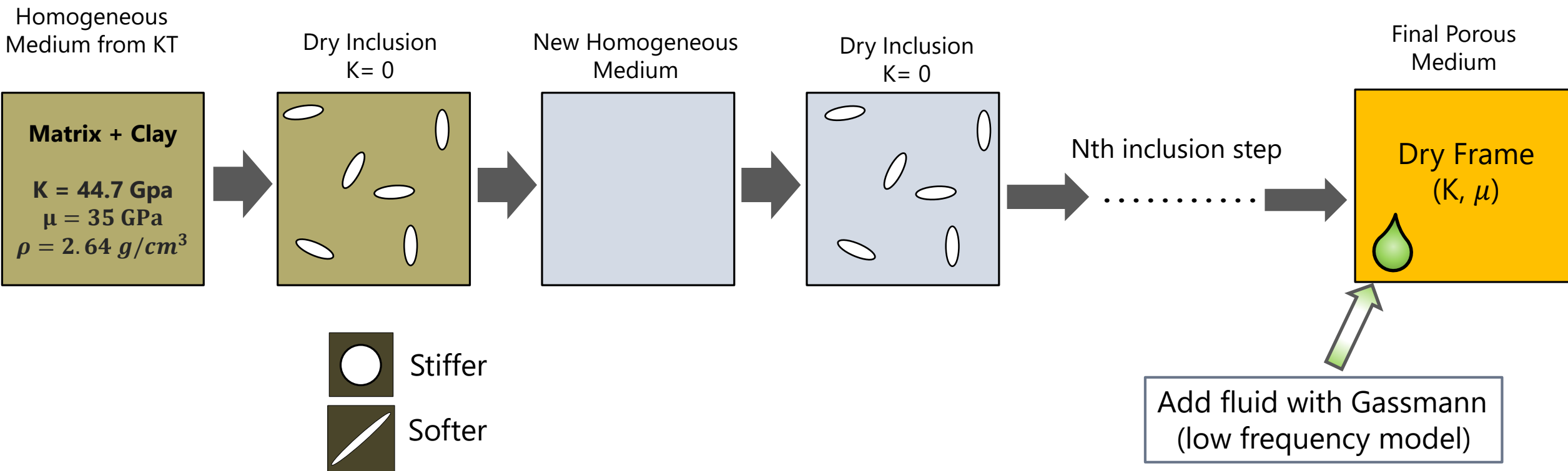


Differential Effective Medium (DEM)

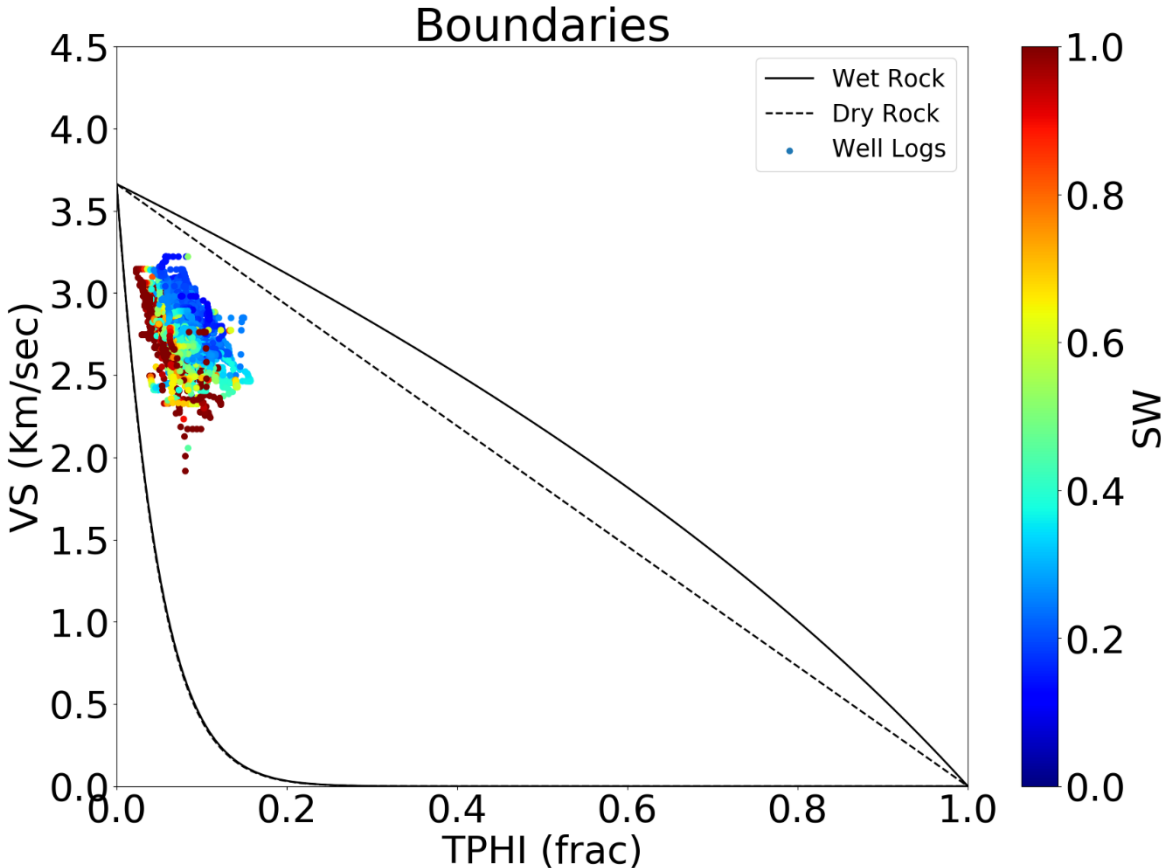
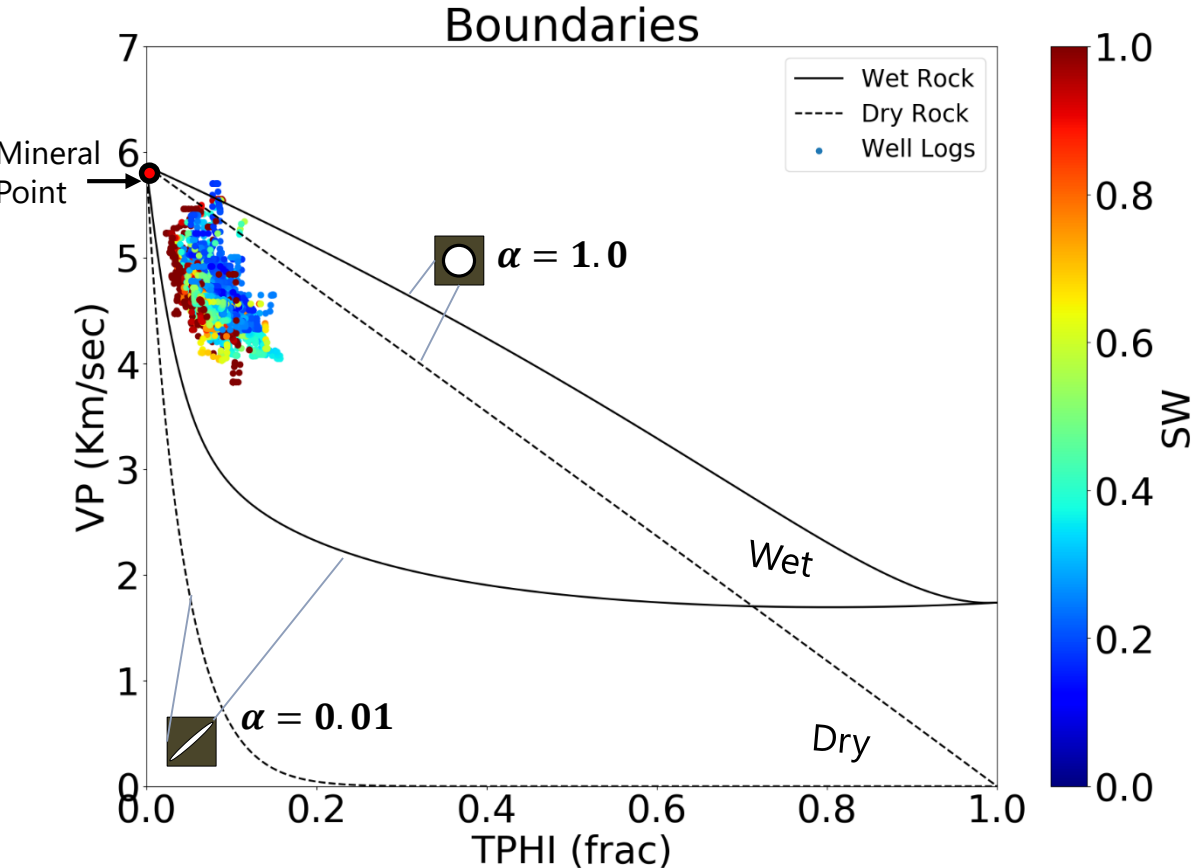
Berryman (1992)

Dry Frame (Add void inclusions)

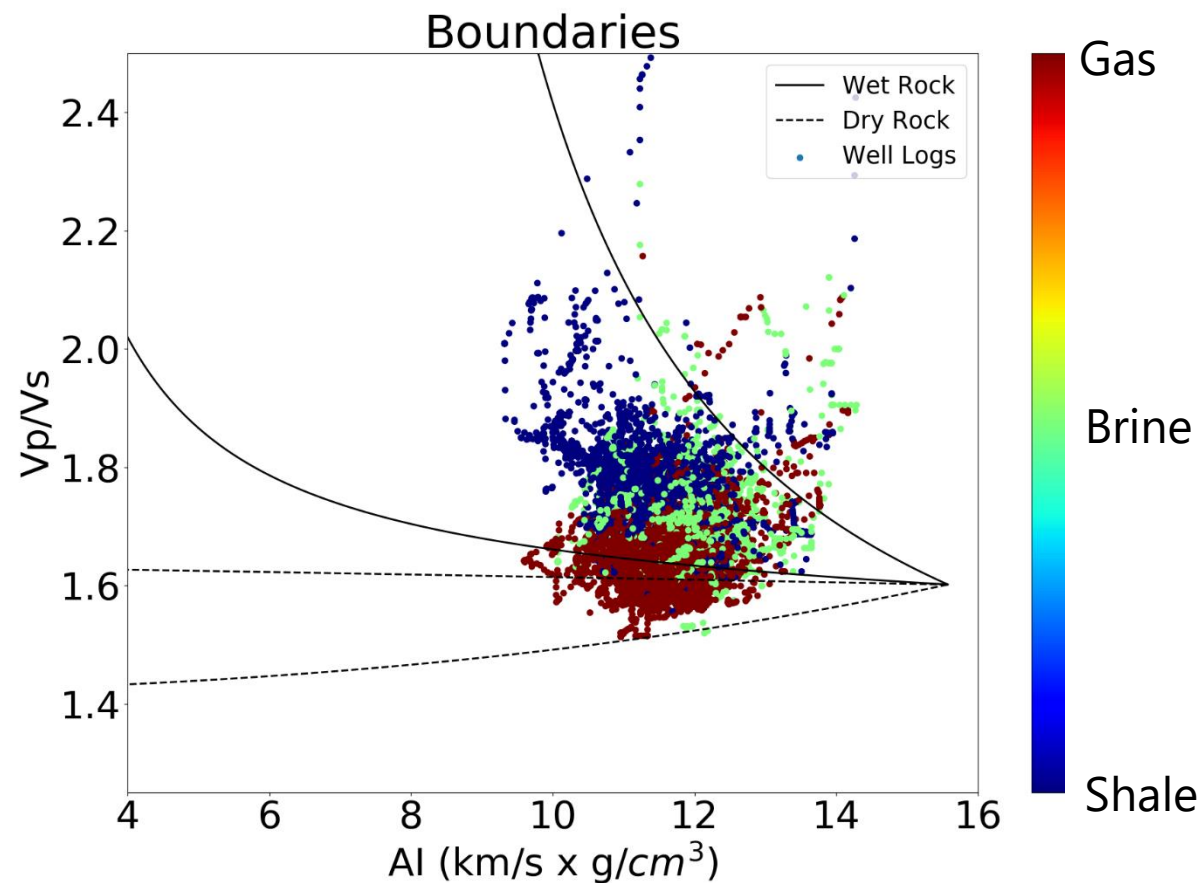
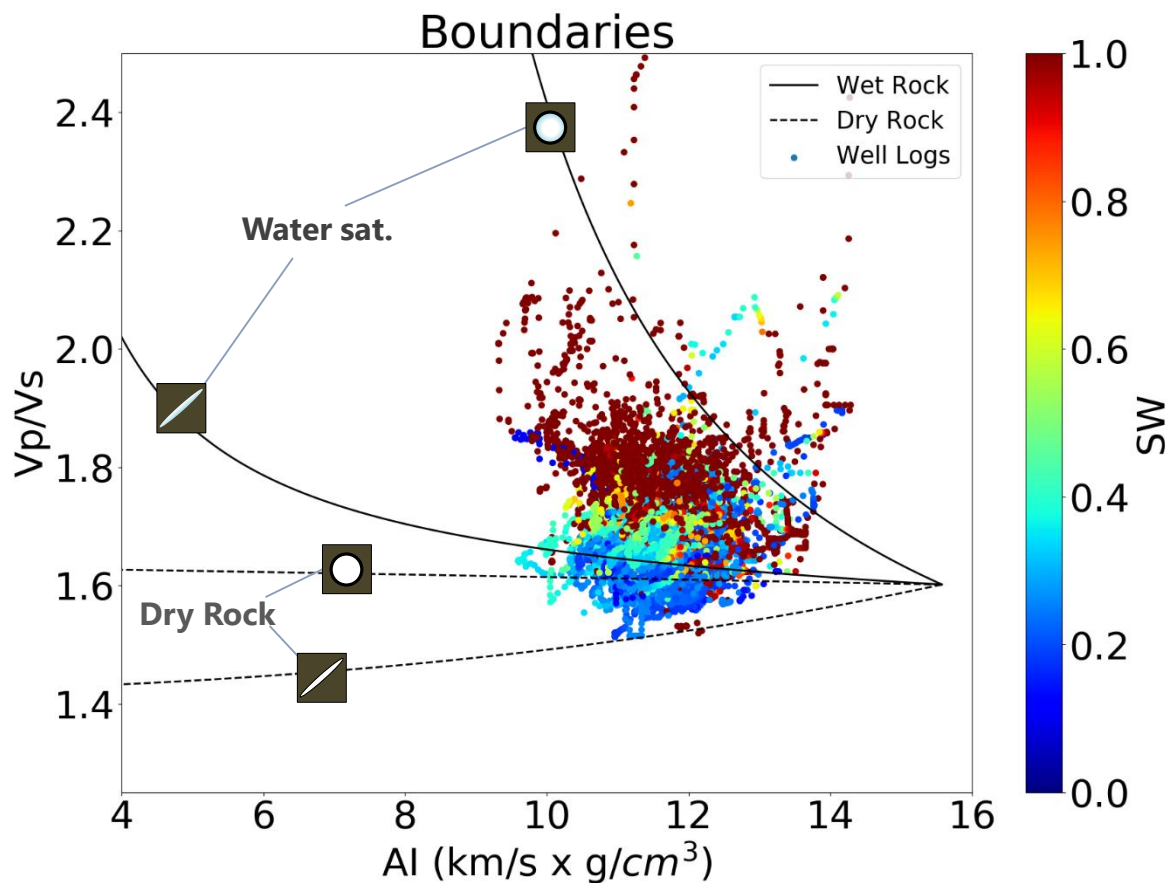
Add inclusions interactively to avoid violating the Kuster and Tuksoz (1974) premises.



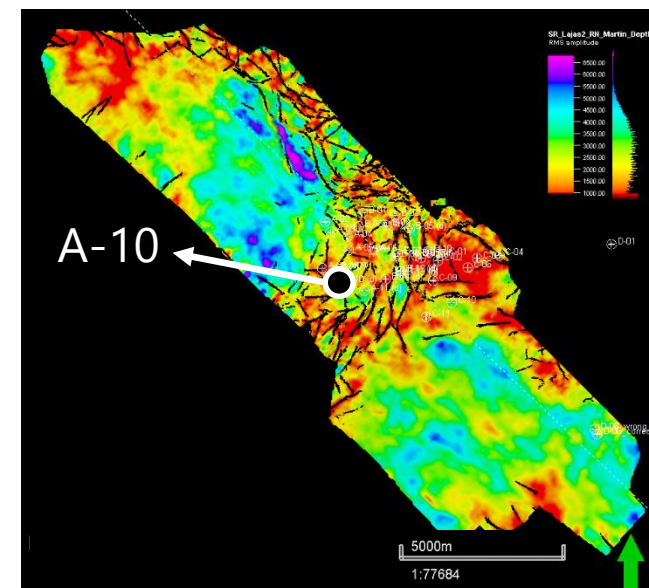
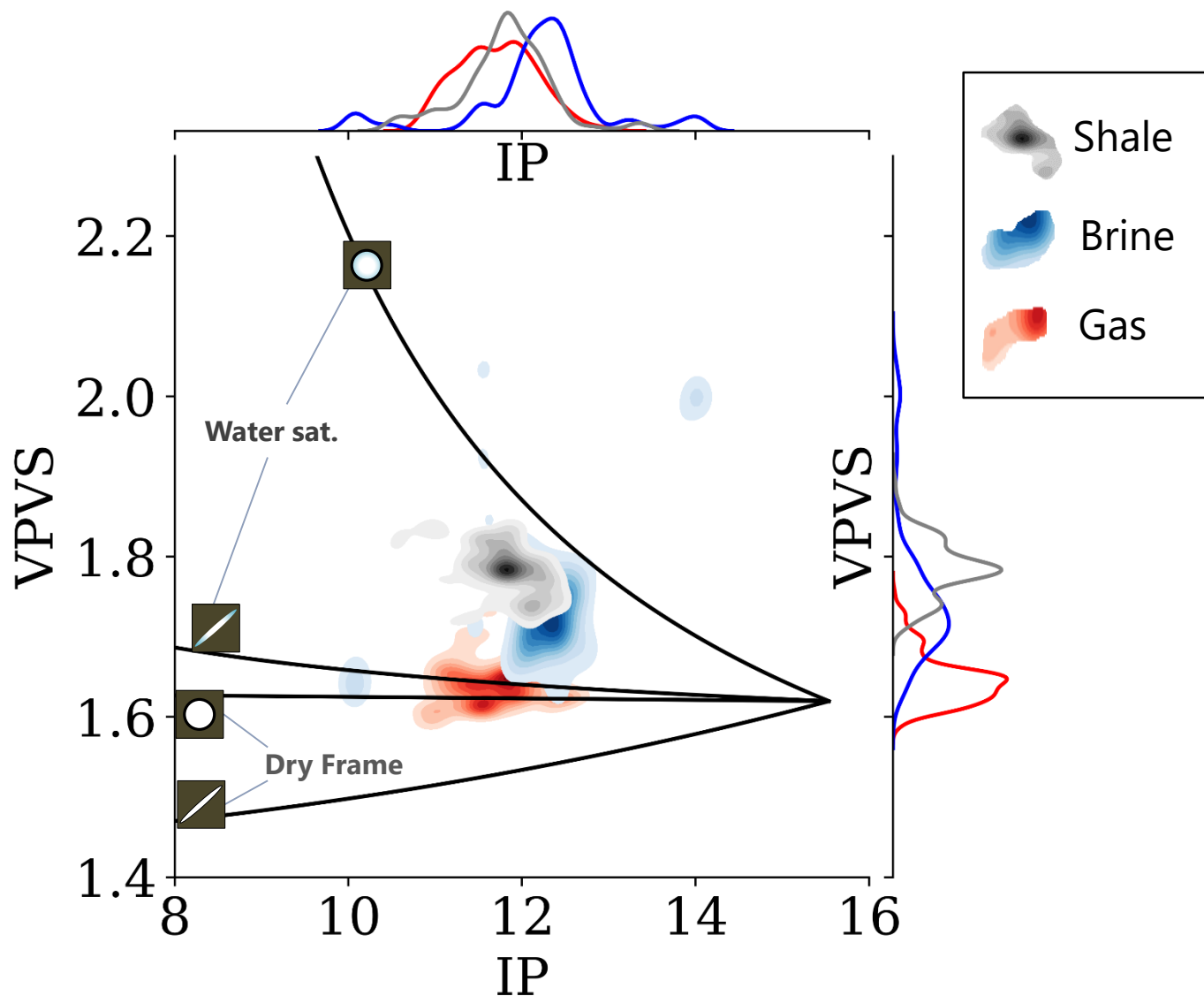
Elastic Moduli Boundaries



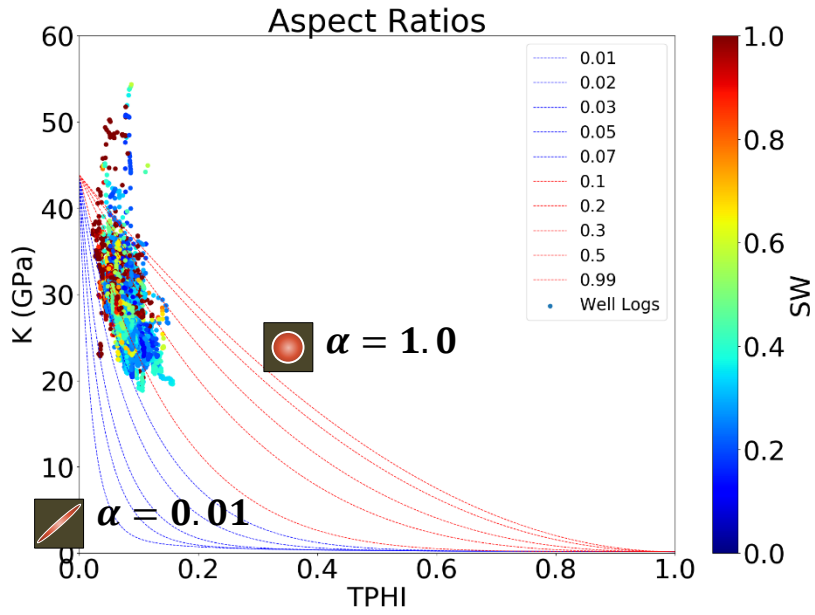
IP x Vp / Vs (Boundaries)



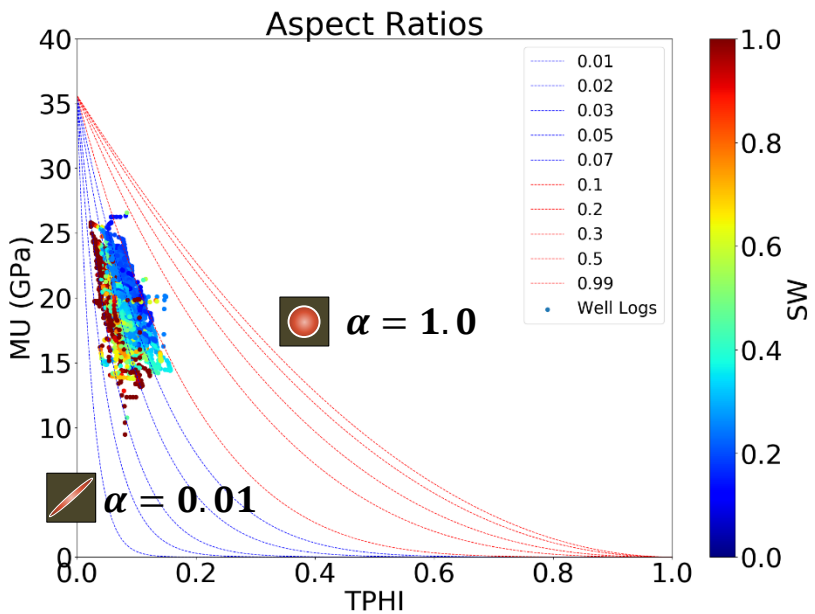
Well A-10



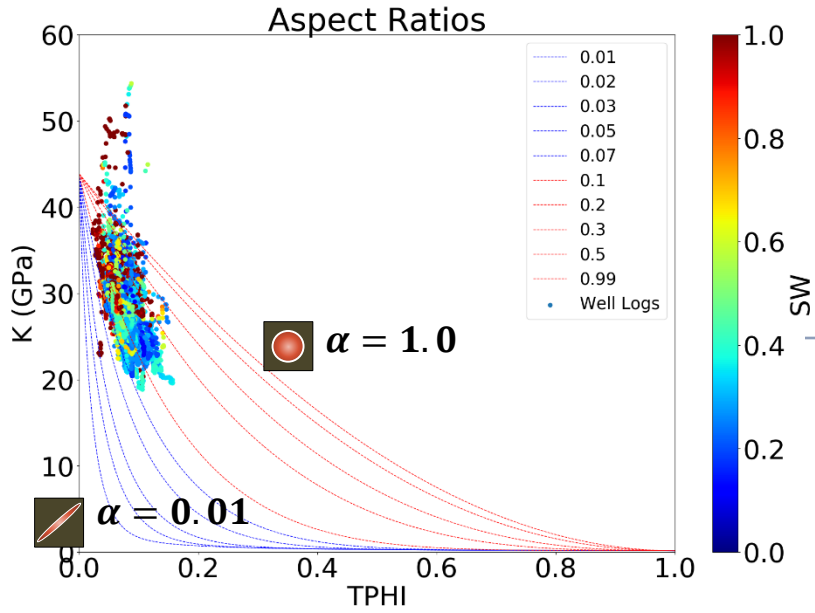
SW: 0 to 100%



Gas Saturated
Medium

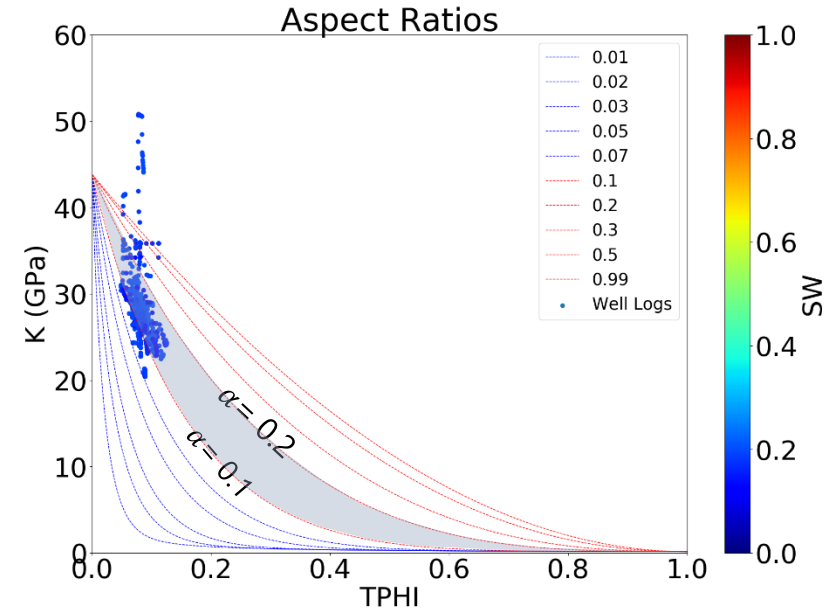


SW: 0 to 100%



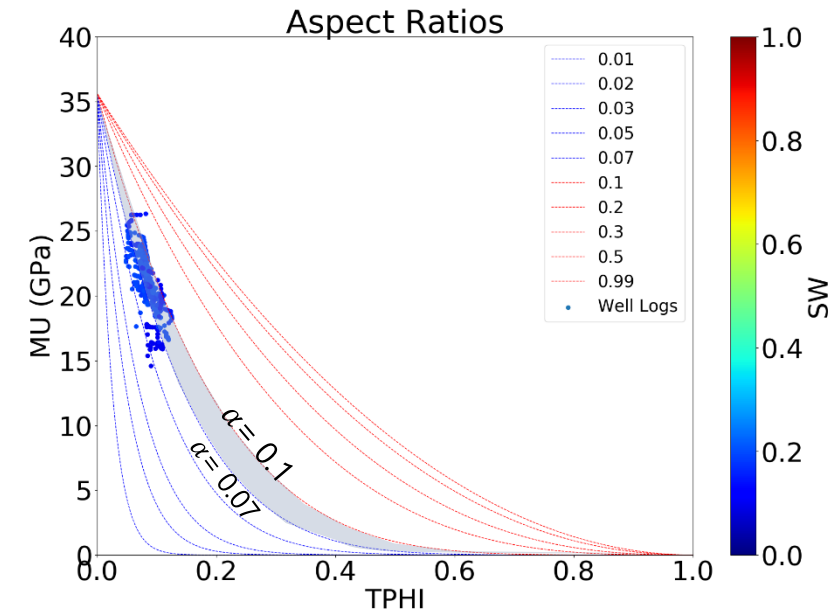
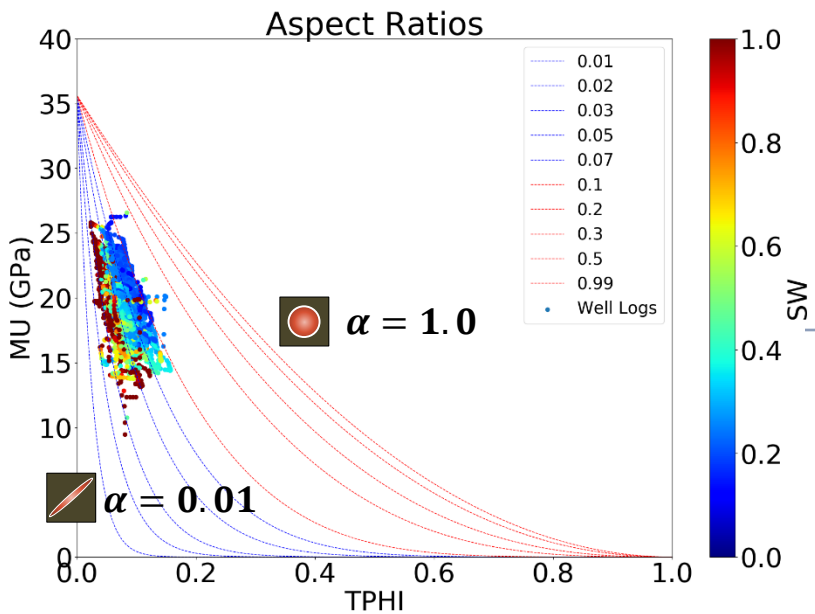
Gas Sandstones

SW: 0 to 20%

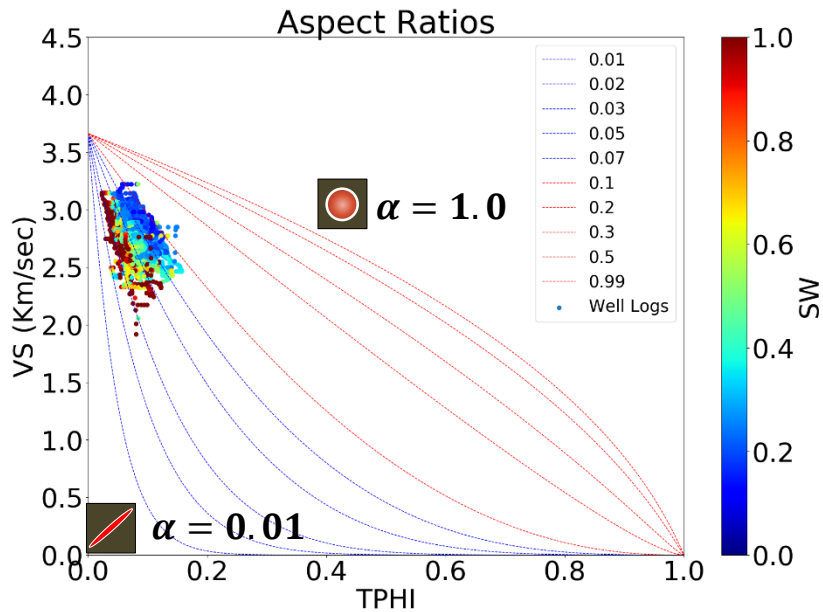
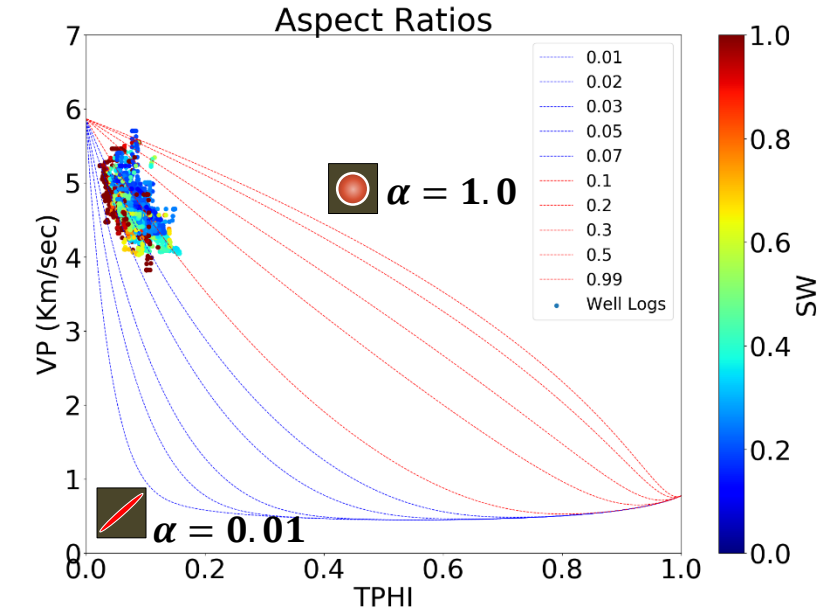


Gas Saturated Medium

$\alpha = 0.07$ to 0.2



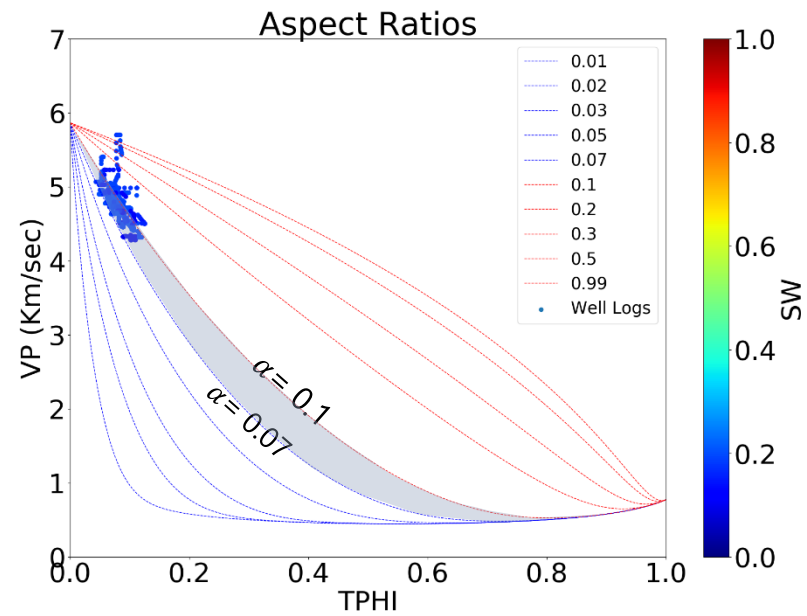
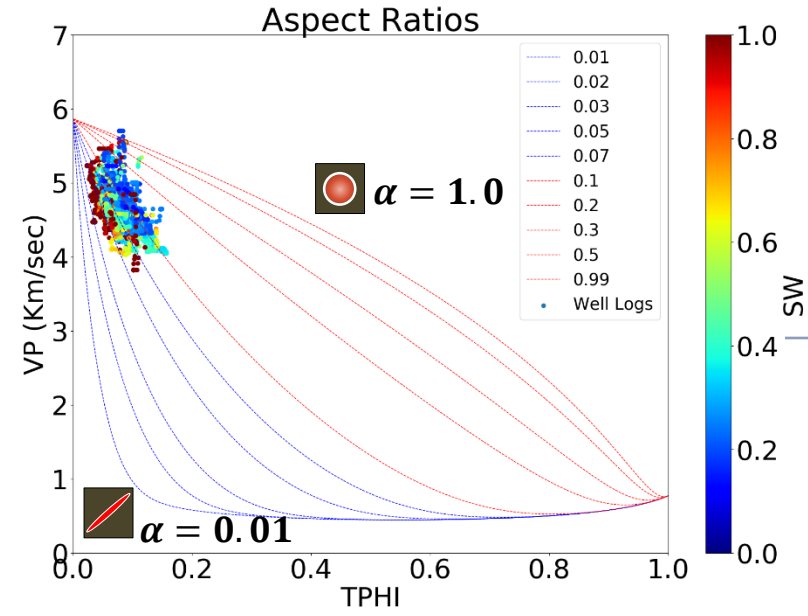
SW: 0 to 100%



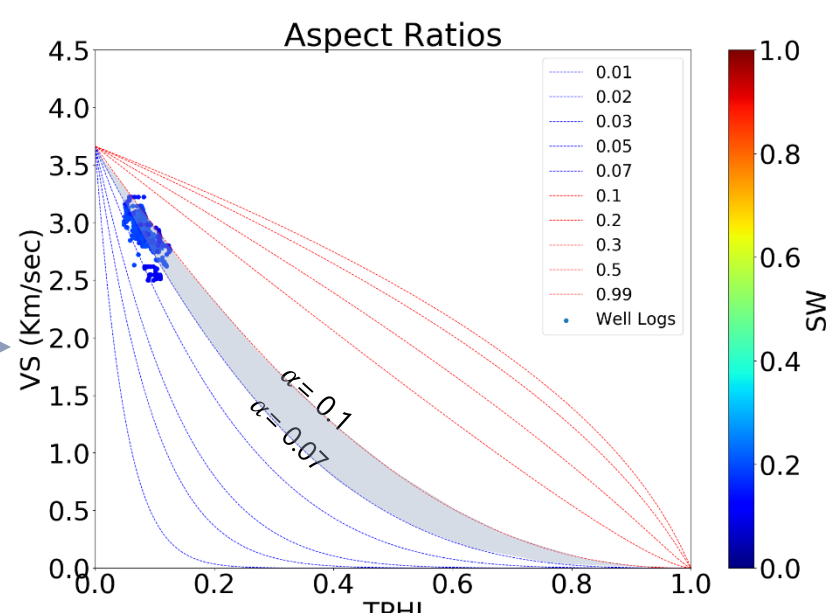
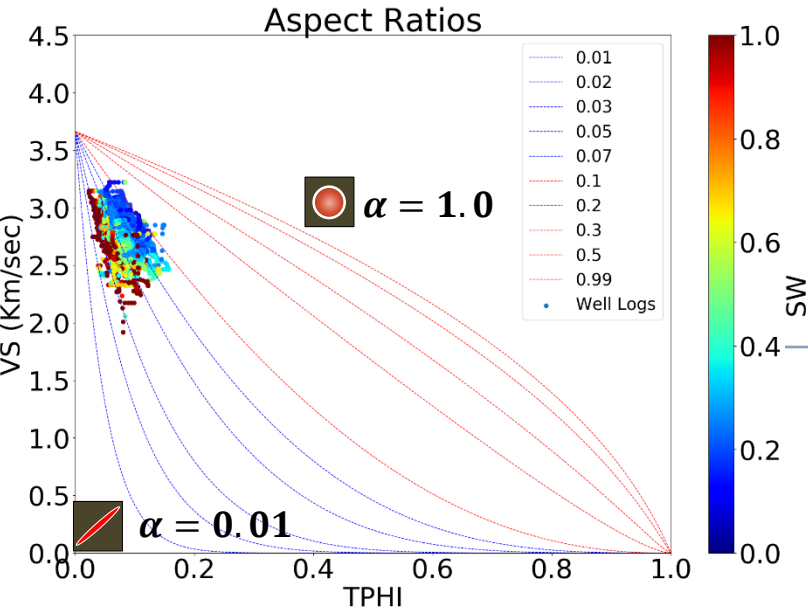
Gas Saturated Medium

SW: 0 to 100%

Gas Sandstones
SW: 0 to 20%

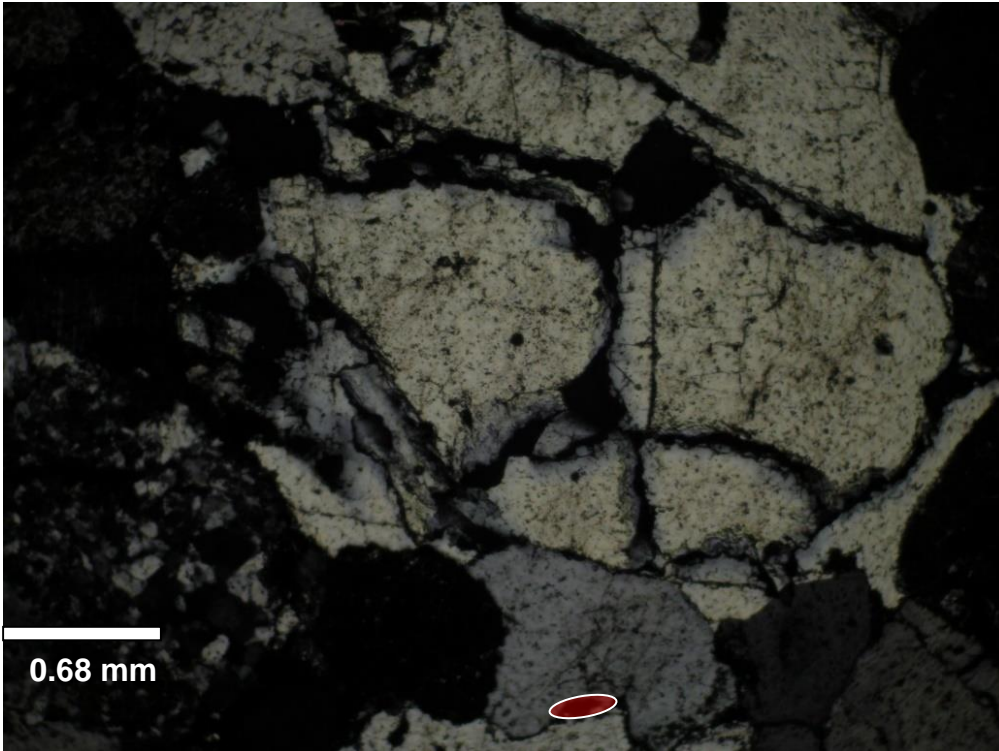


Gas Saturated Medium

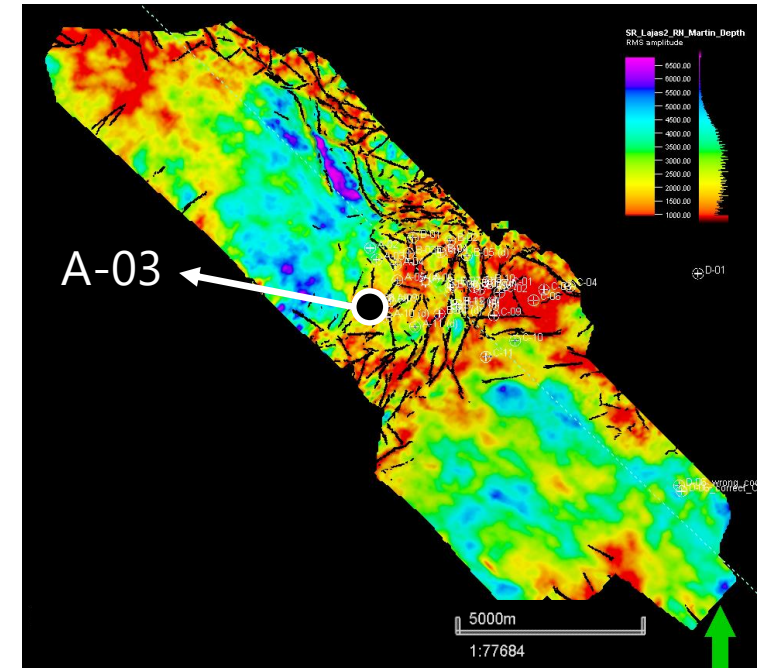


$\alpha = 0.07$ to 0.1

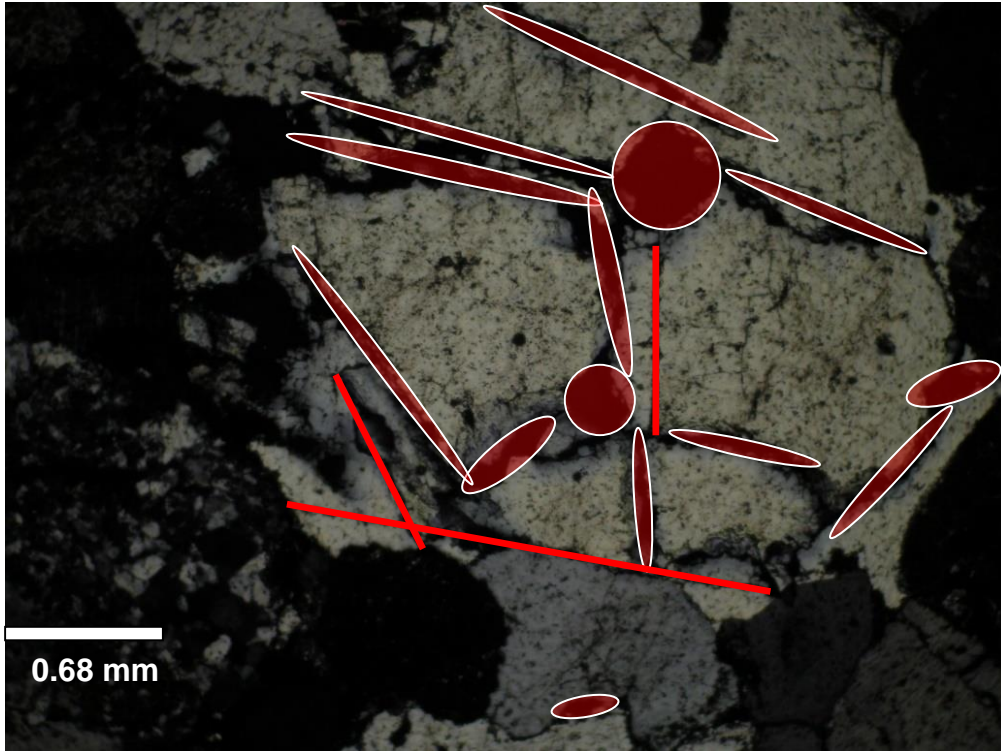
$\alpha = 0.2$ (average)



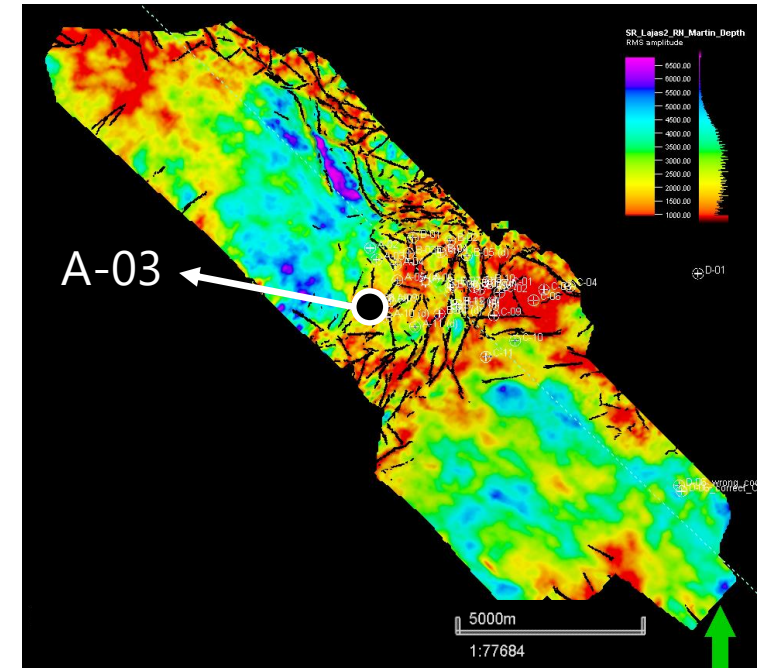
A-03. Dissolution of Feldspars and microfractures

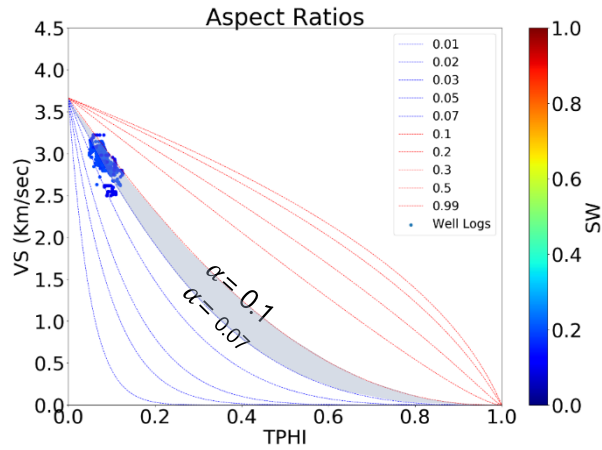


$\alpha = 0.15$ (average)



A-03. Dissolution of Feldspars and microfractures





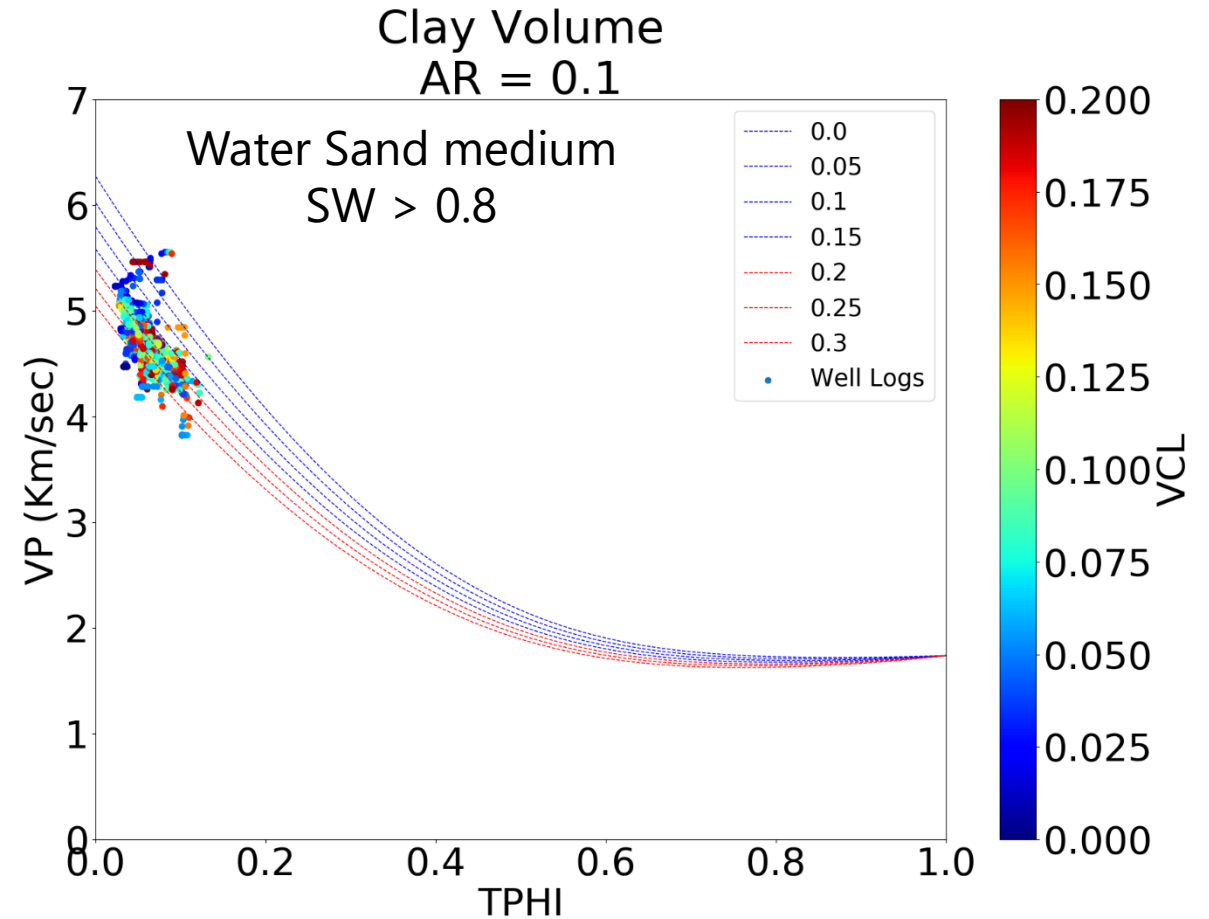
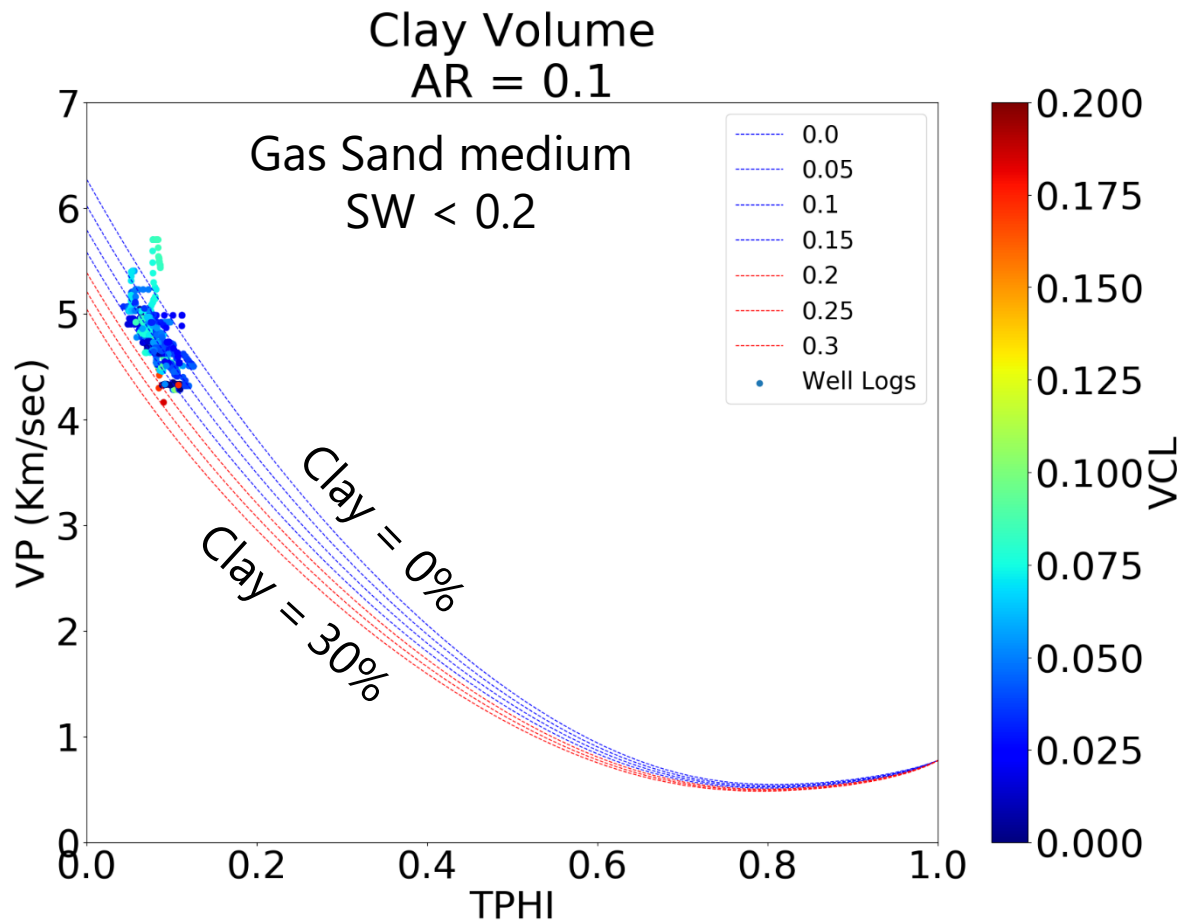
$\alpha = 0.07$ to 0.2
Best fit for the model
(based on xplot analysis)



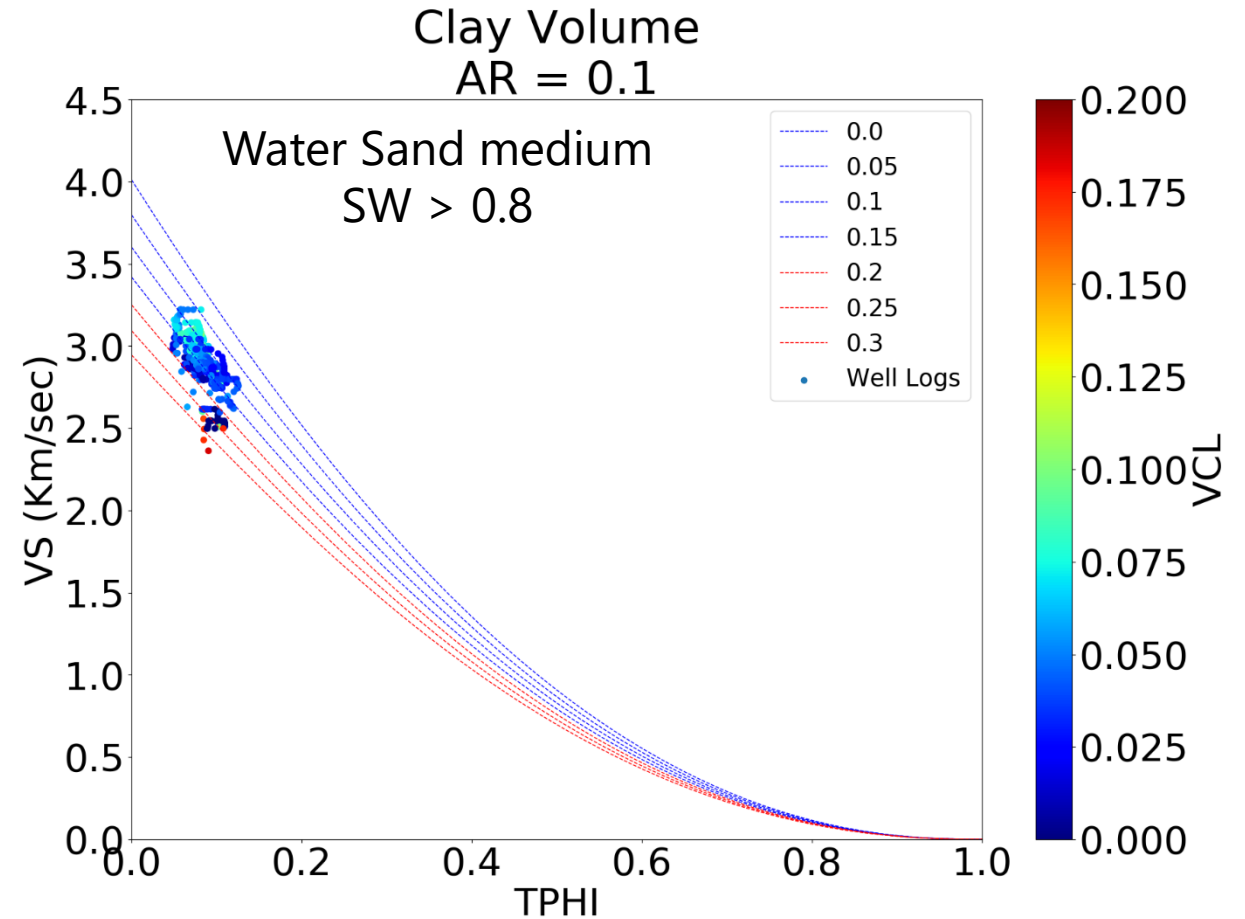
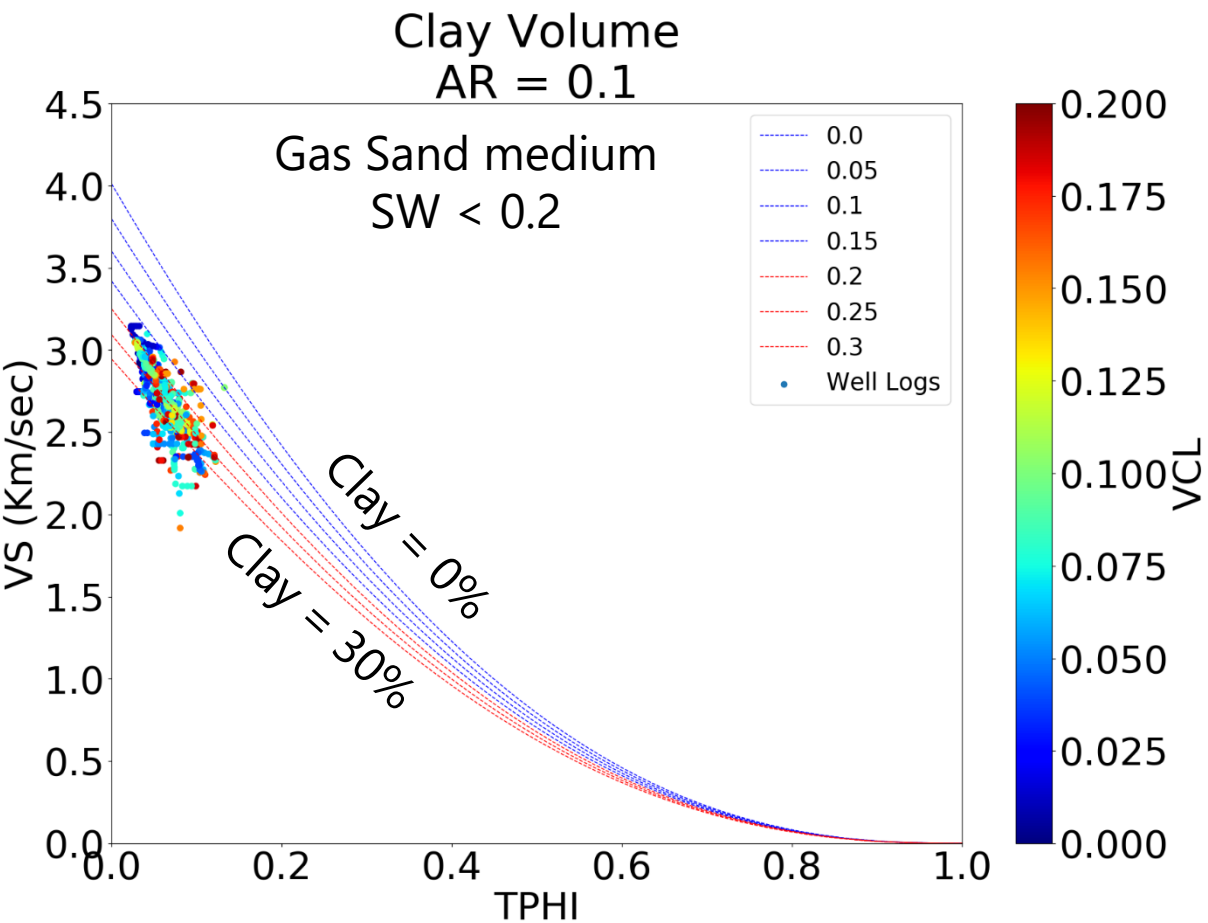
$\alpha = 0.15$

$\alpha_{ref} = 0.1$

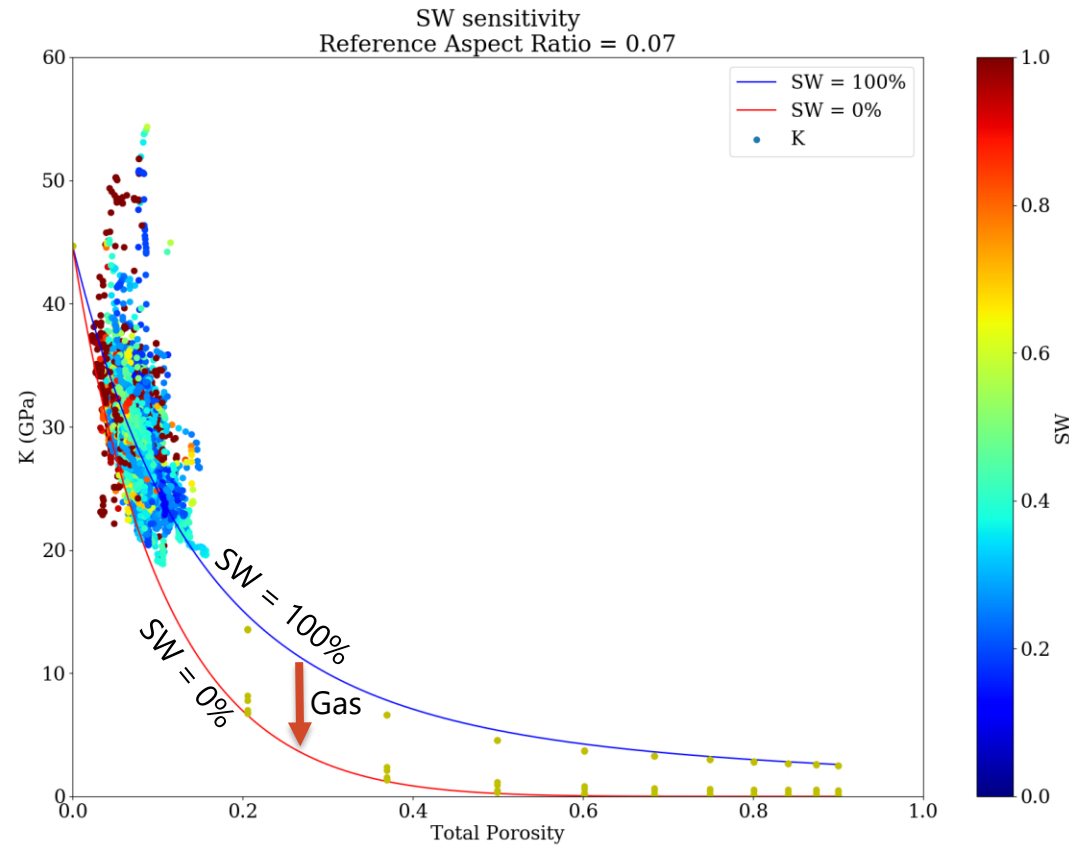
Clay Analysis - VP



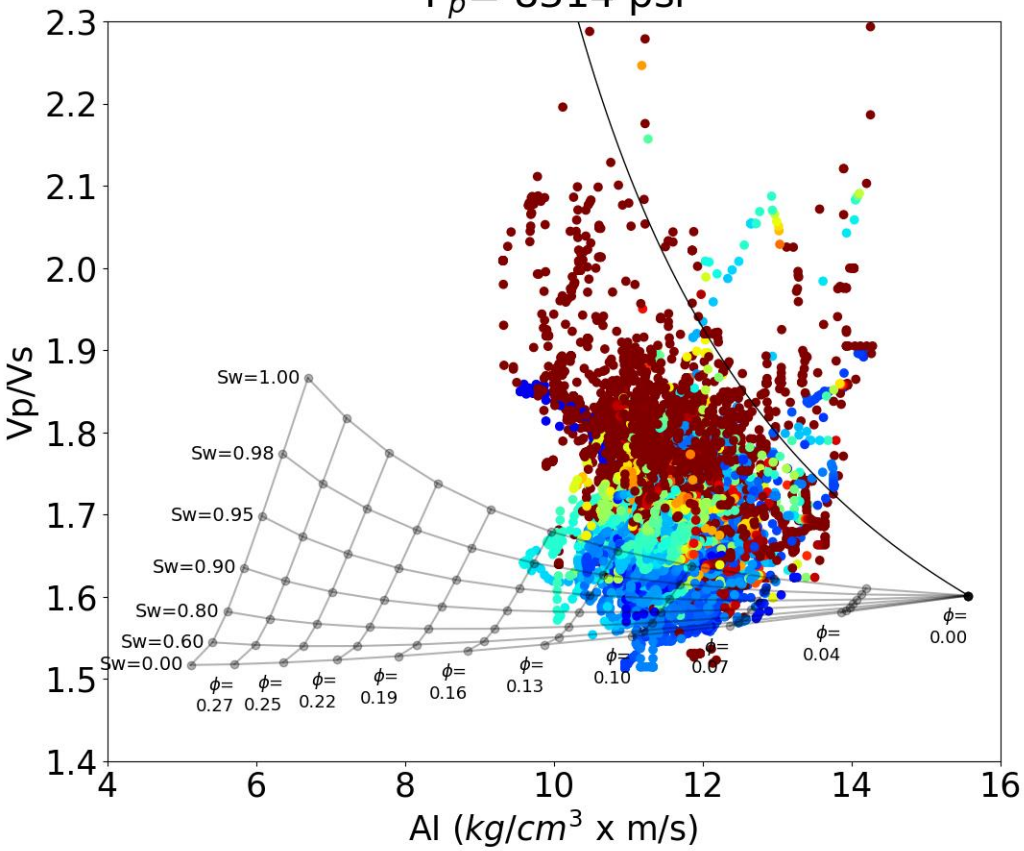
Clay Analysis - VS



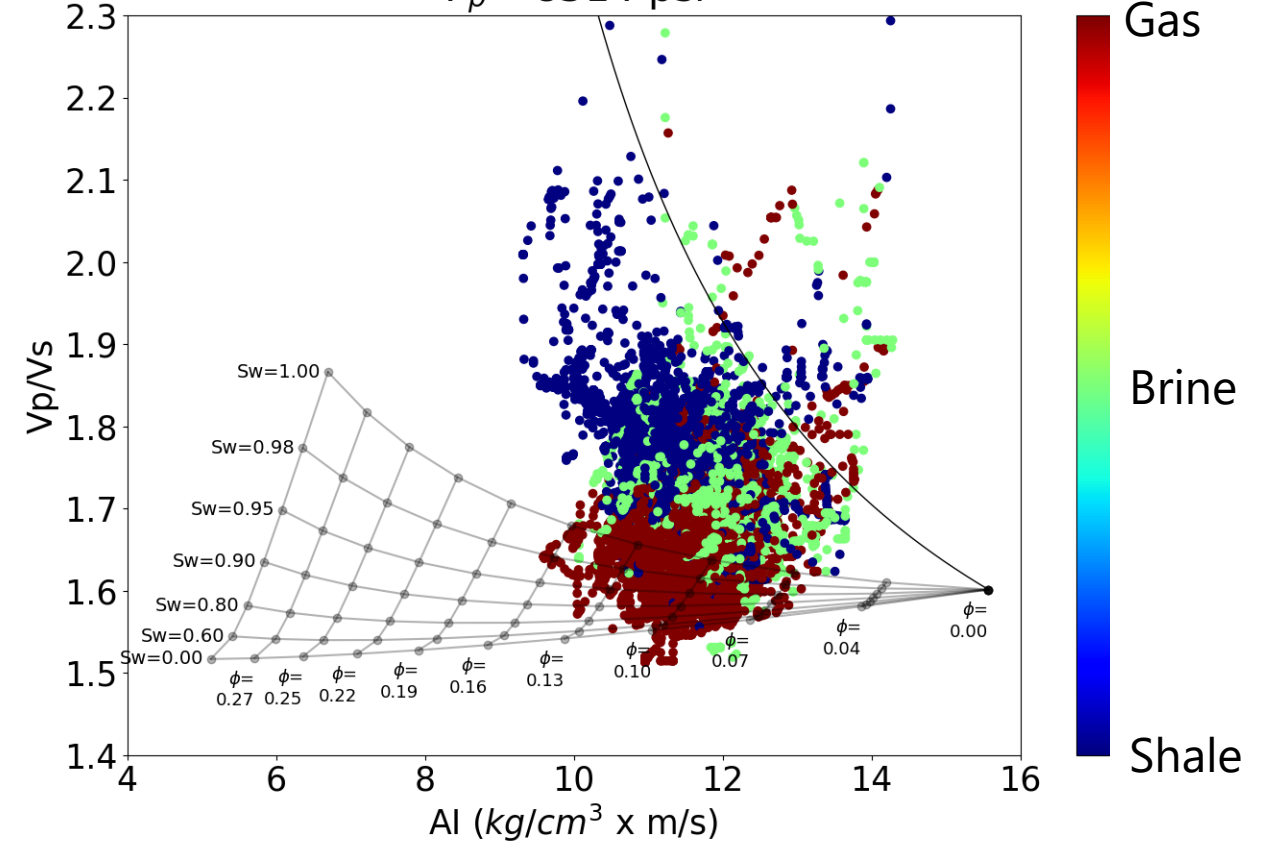
Water Saturation Sensitivity

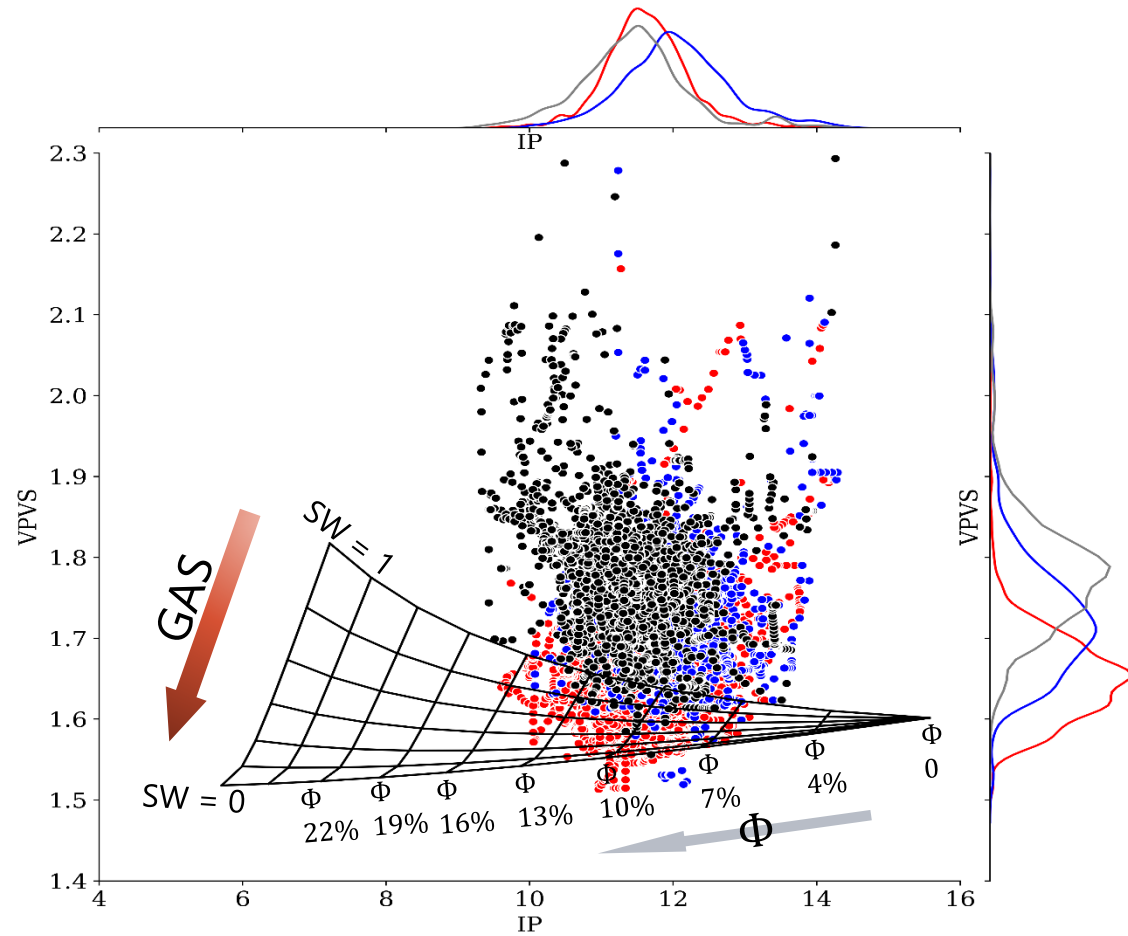


$AR_{ref} = 0.1$
 $P_p = 8314$ psi



$AR_{ref} = 0.1$
 $P_p = 8314$ psi





Conclusions and Future Works

- Pre stack inversion is necessary to identify the gas zones
- The rock physics model based in the pore shape can model the seismic response of the tight sand of the Lajas Formation.

Conclusions and Future Works

Improve the model

- Effect of pressure on the Dry Frame
- Clays properties
- Bounded water (irreplaceable constituent of the matrix)

Punta Rosada Fomation

Post and Pre stack Inversion



Back-up slides

Kuster and Toksöz (1974) derived expressions for P- and S- wave velocities by using a long-wavelength first-order scattering theory. A generalization of their expressions for the effective moduli K_{KT}^* and μ_{KT}^* for a variety of inclusion shapes can be written as (Kuster and Toksöz, 1974; Berryman, 1980b)

$$(K_{KT}^* - K_m) \frac{(K_m + \frac{4}{3}\mu_m)}{(K_{KT}^* + \frac{4}{3}\mu_m)} = \sum_{i=1}^N x_i (K_i - K_m) P^{mi}$$

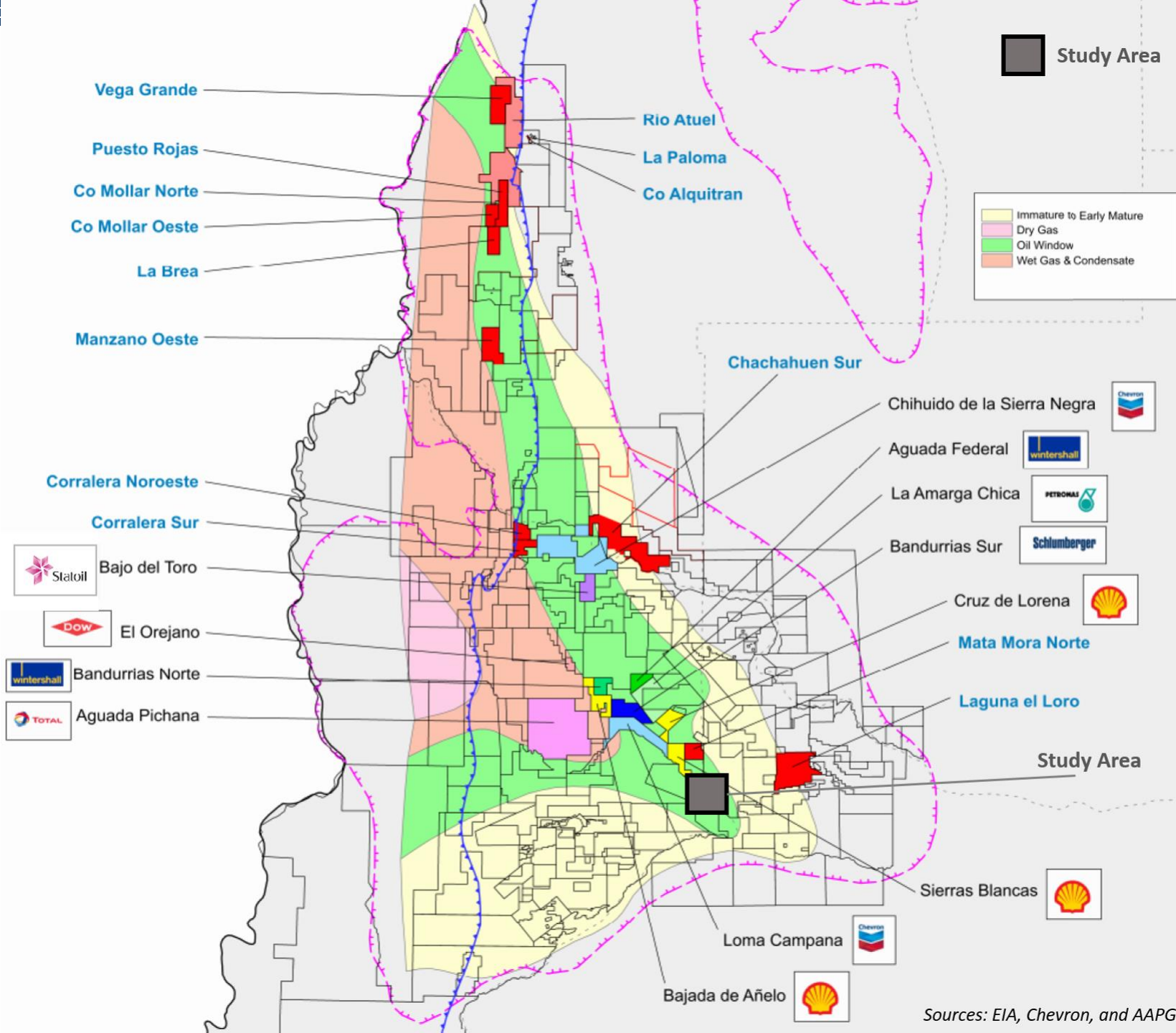
$$(\mu_{KT}^* - \mu_m) \frac{(\mu_m + \zeta_m)}{(\mu_{KT}^* + \zeta_m)} = \sum_{i=1}^N x_i (\mu_i - \mu_m) Q^{mi}$$

where the summation is over the different inclusion types with volume concentration x_i , and

$$\zeta = \frac{\mu (9K + 8\mu)}{6 (K + 2\mu)}$$

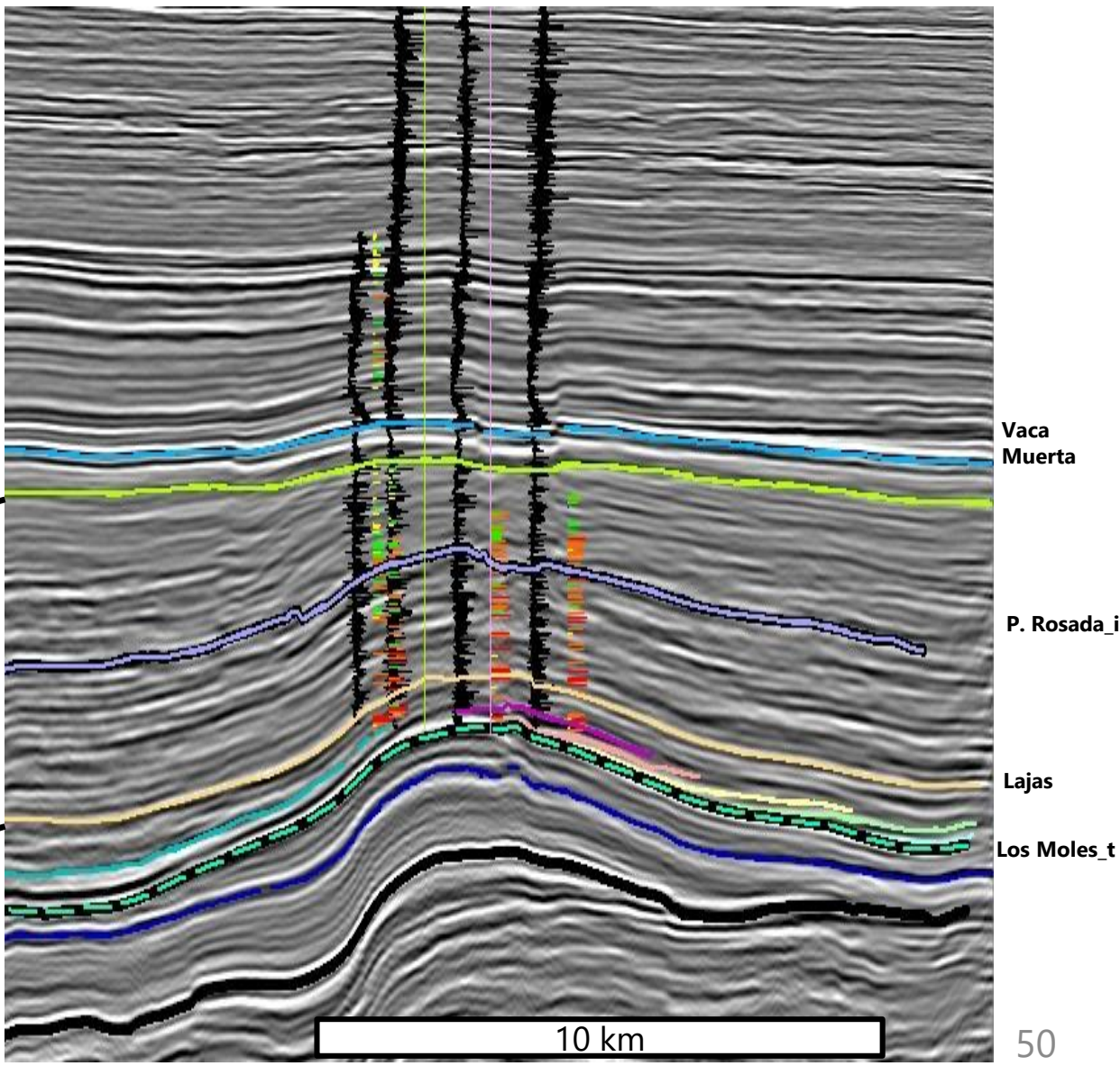
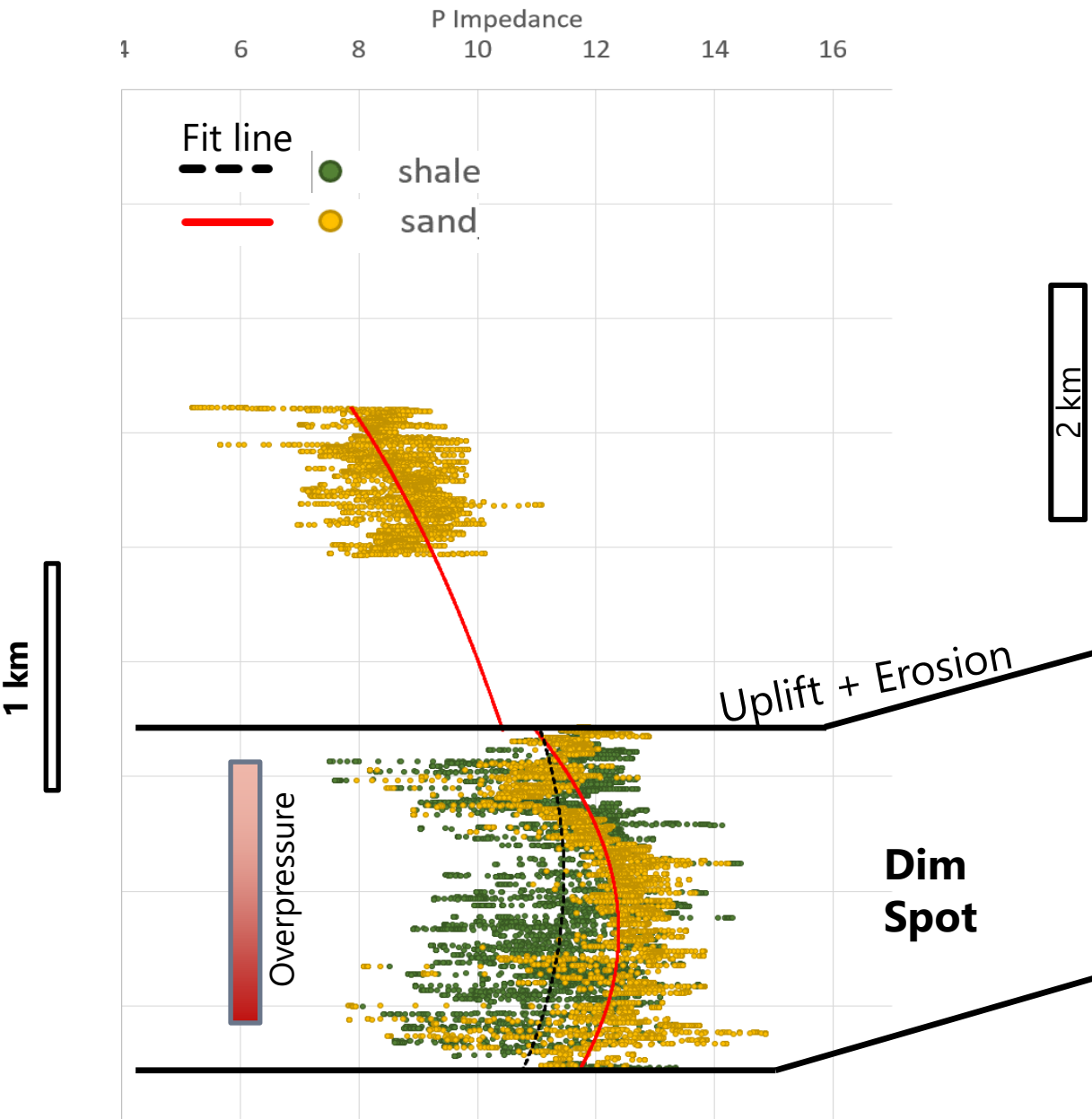
TABLE 4.7.1. Coefficients P and Q for some specific shapes. The subscripts m and i refer to the background and inclusion materials [from Berryman (1995)].

| Inclusion Shape | P^{mi} | Q^{mi} |
|-----------------|--|---|
| Spheres | $\frac{K_m + \frac{4}{3}\mu_m}{K_i + \frac{4}{3}\mu_m}$ | $\frac{\mu_m + \zeta_m}{\mu_i + \zeta_m}$ |
| Needles | $\frac{K_m + \mu_m + \frac{1}{3}\mu_i}{K_i + \mu_m + \frac{1}{3}\mu_i}$ | $\frac{1}{5} \left(\frac{4\mu_m}{\mu_m + \mu_i} + 2 \frac{\mu_m + \gamma_m}{\mu_i + \gamma_m} + \frac{K_i + \frac{4}{3}\mu_m}{K_i + \mu_m + \frac{1}{3}\mu_i} \right)$ |
| Disks | $\frac{K_m + \frac{4}{3}\mu_i}{K_i + \frac{4}{3}\mu_i}$ | $\frac{\mu_m + \zeta_i}{\mu_i + \zeta_i}$ |
| Penny cracks | $\frac{K_m + \frac{4}{3}\mu_i}{K_i + \frac{4}{3}\mu_i + \pi\alpha\beta_m}$ | $\frac{1}{5} \left(1 + \frac{8\mu_m}{4\mu_i + \pi\alpha(\mu_m + 2\beta_m)} + 2 \frac{K_i + \frac{2}{3}(\mu_i + \mu_m)}{K_i + \frac{4}{3}\mu_i + \pi\alpha\beta_m} \right)$ |

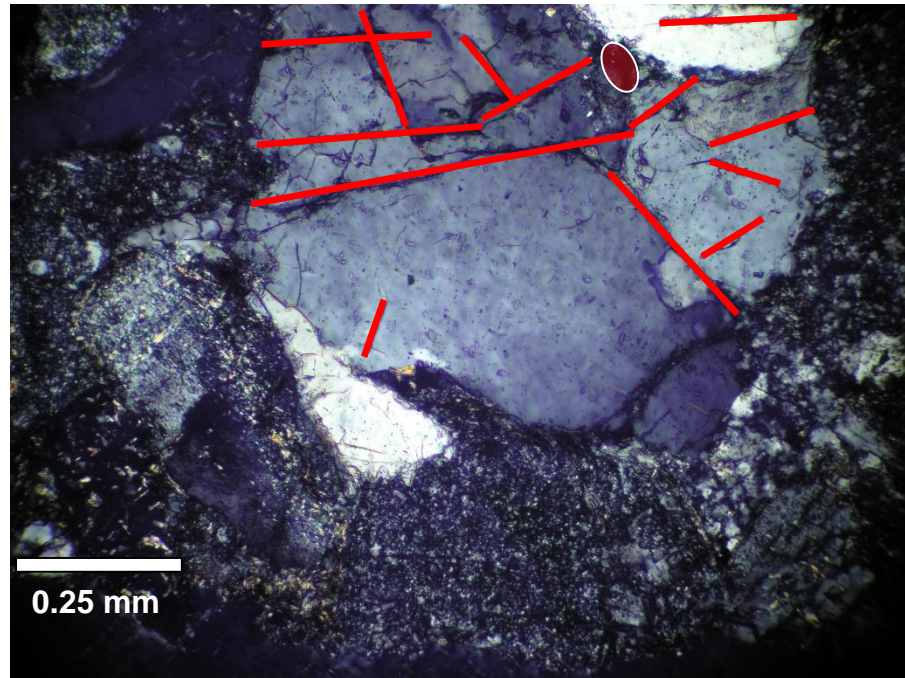


Sources: EIA, Chevron, and AAPG.

Compaction



$\alpha = 0.01$ (average)



A-06. Microfractures

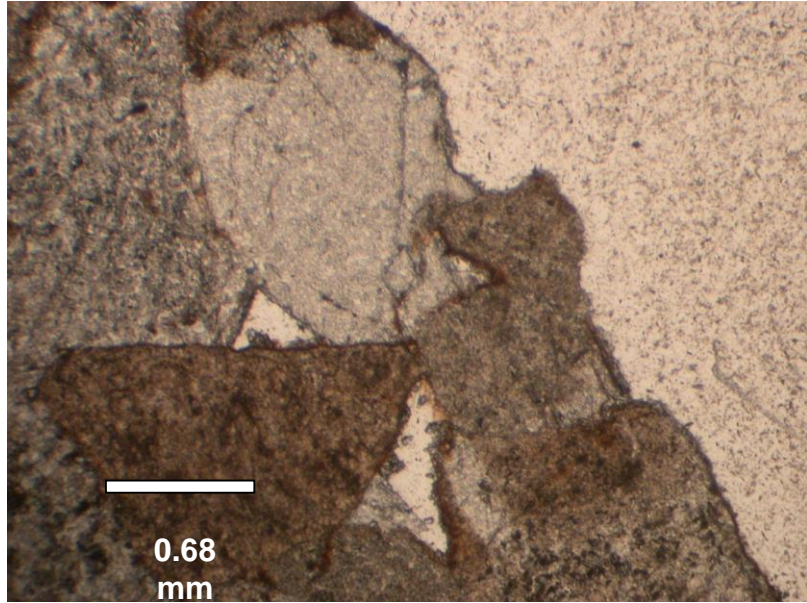


Foto 16: RN 1007 3620 x4 compactación.;
crecimiento secundario de cuarzo.

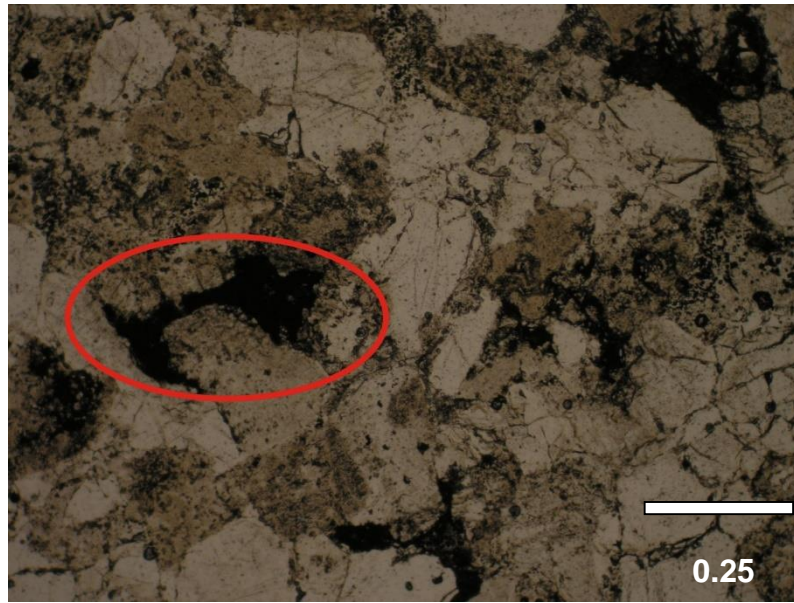


Foto 134 RN 1040 3332,50 x10 *voids* ocluidos con
materia orgánica.

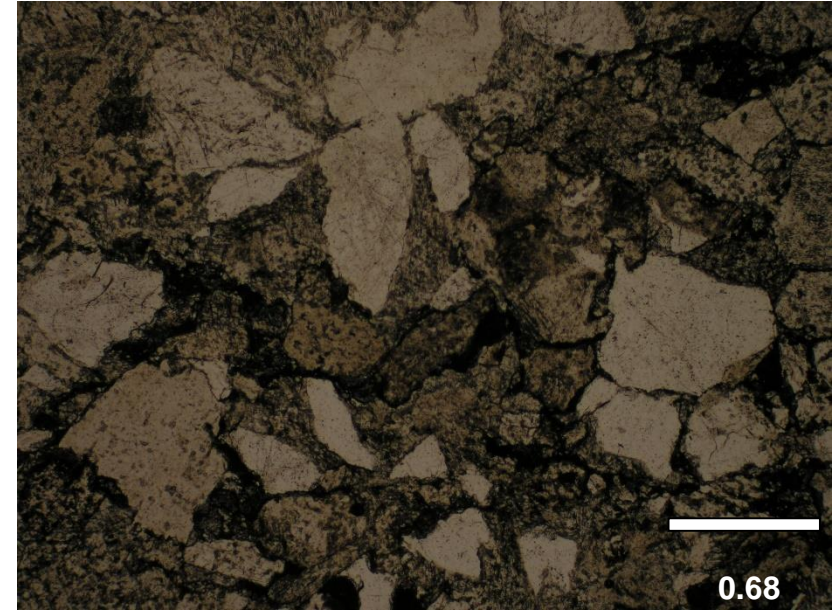


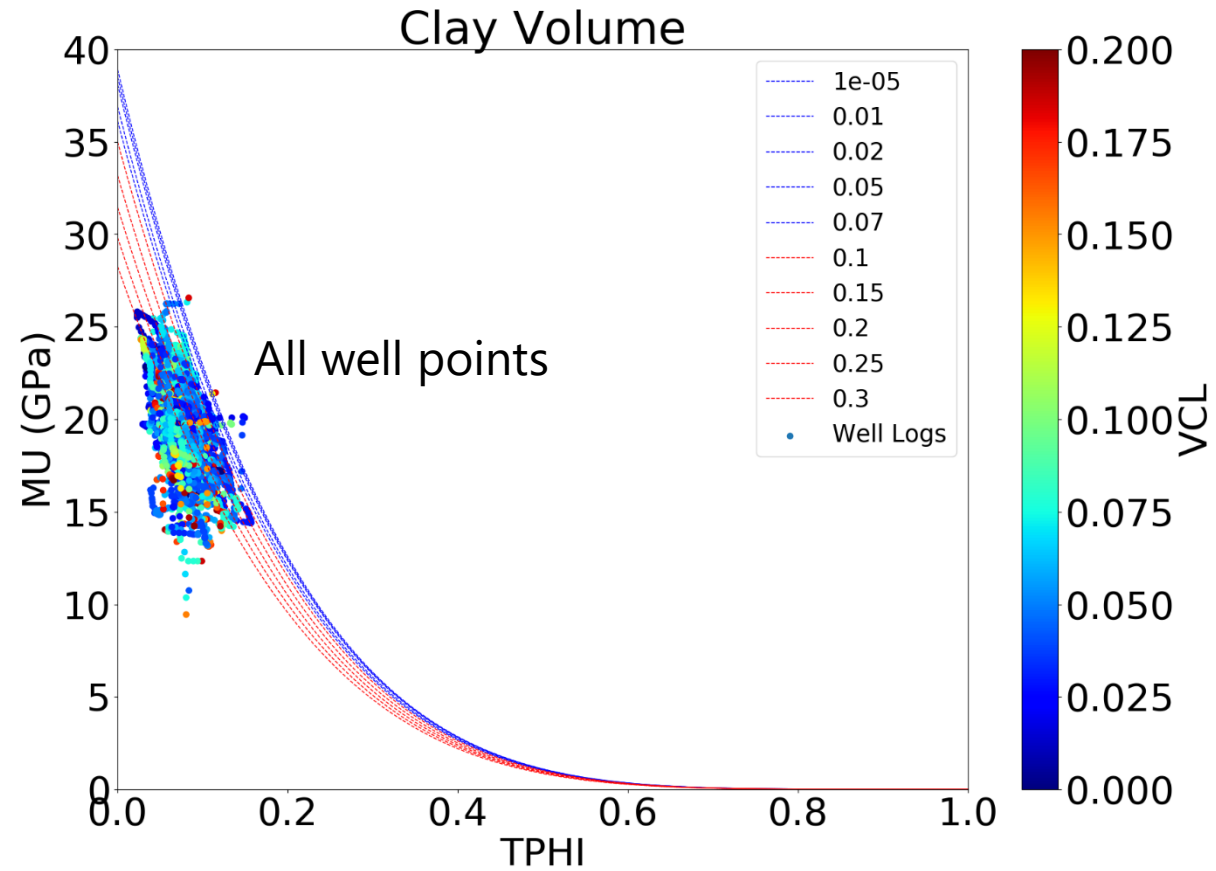
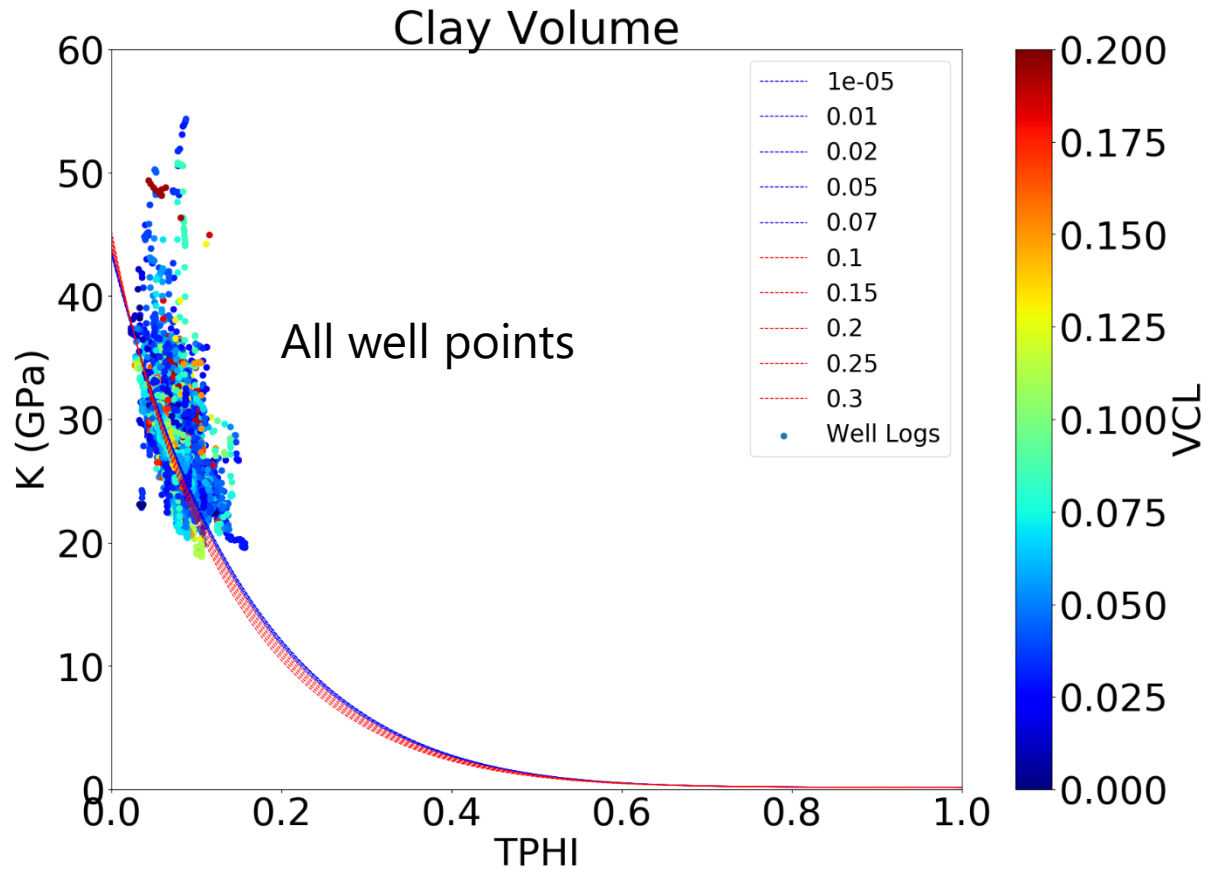
Foto 139 RN 252 3397,38 x4XN materia orgánica en
fracturas.

Clay Analysis

Water Saturated media

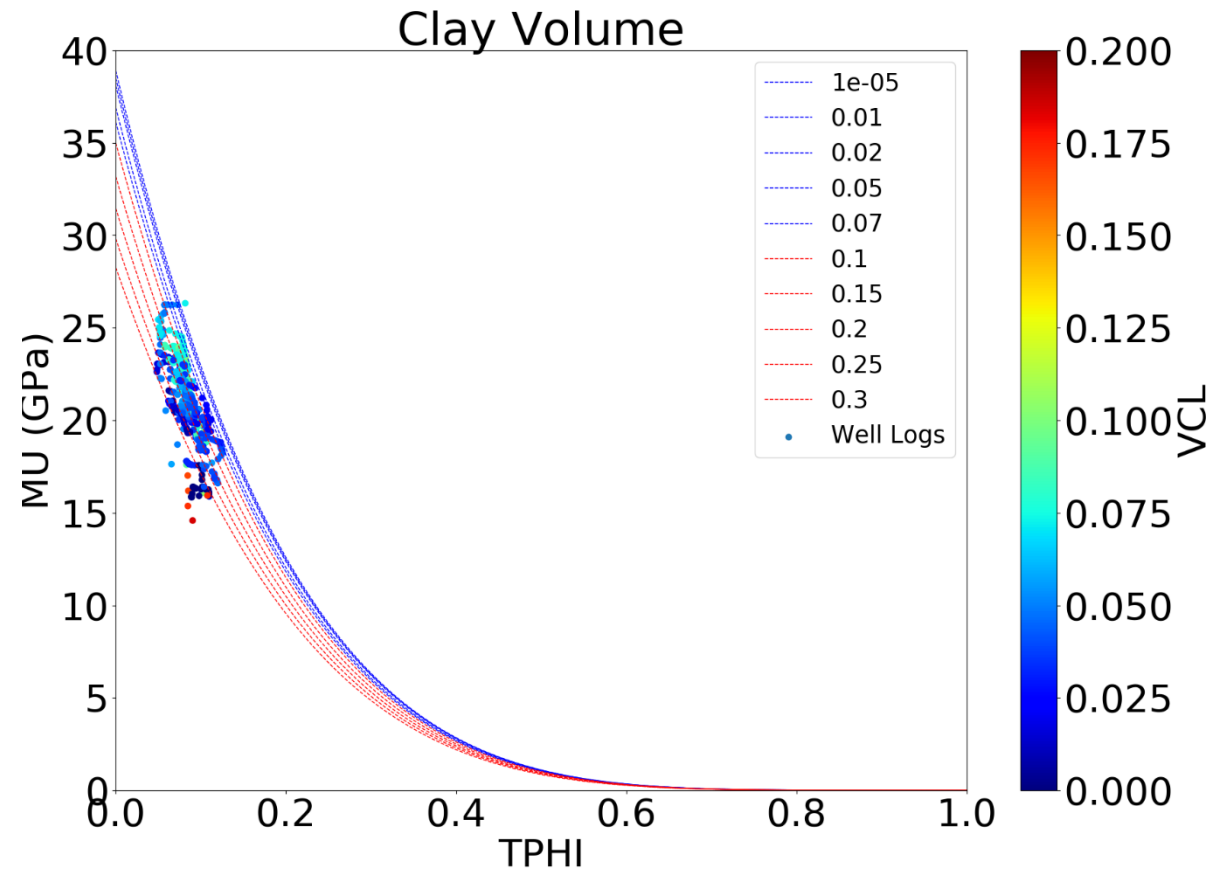
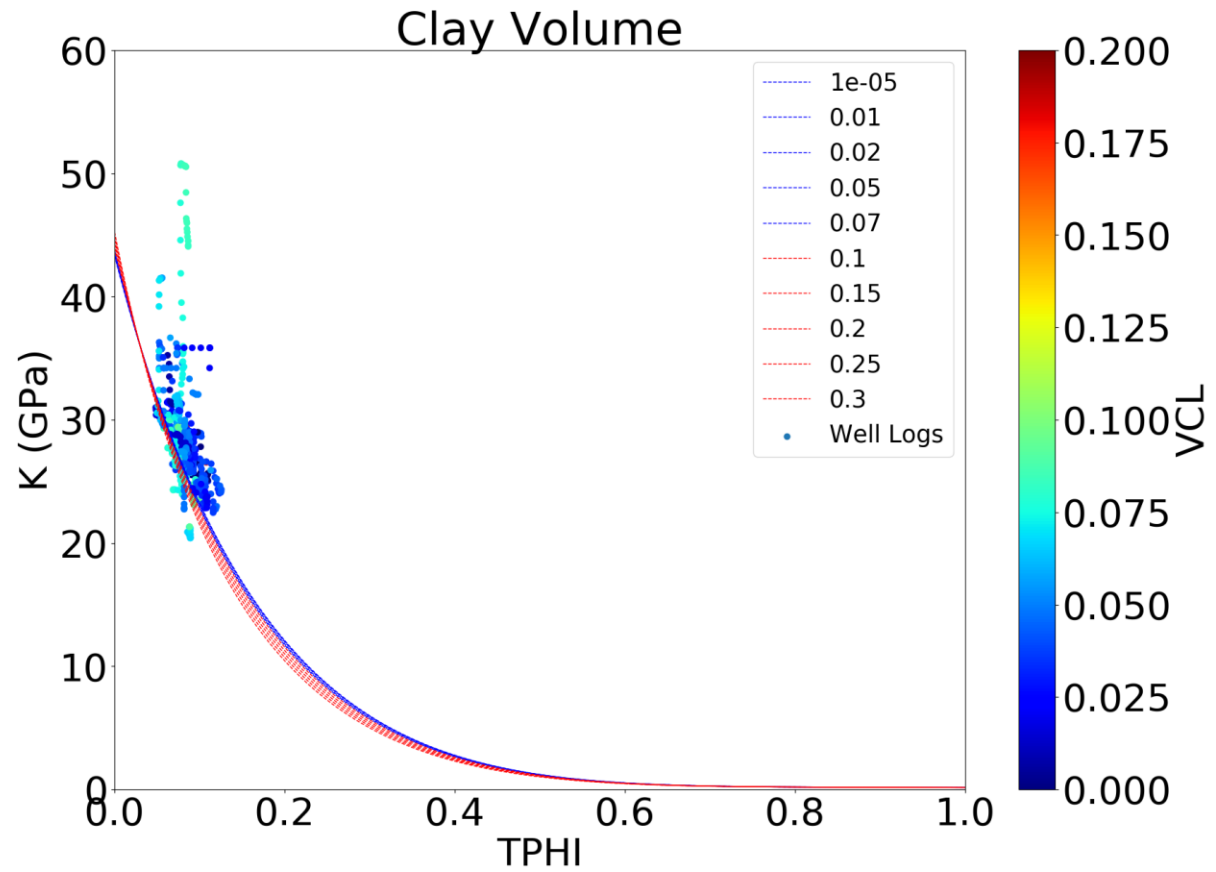
$$\alpha = 0.1$$

All well points

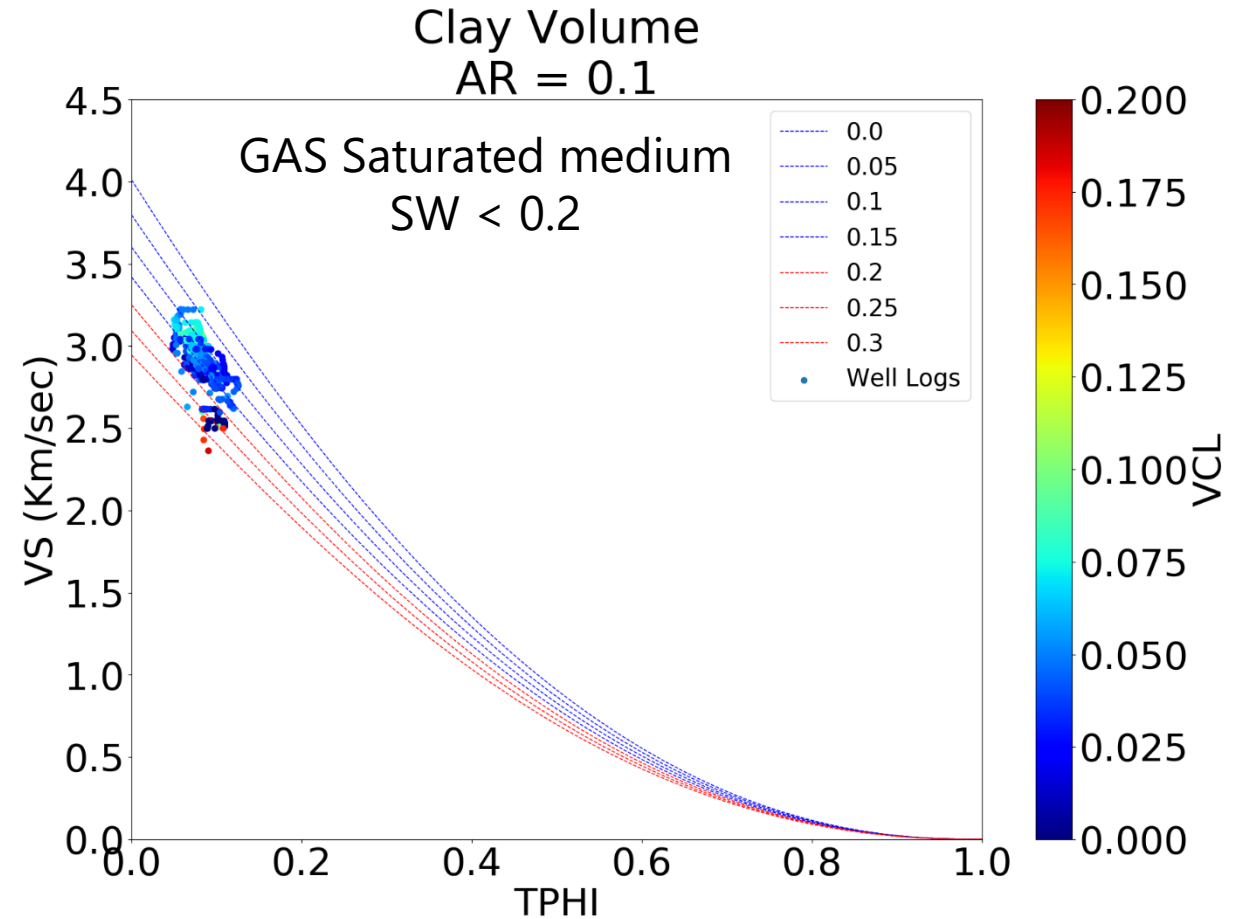
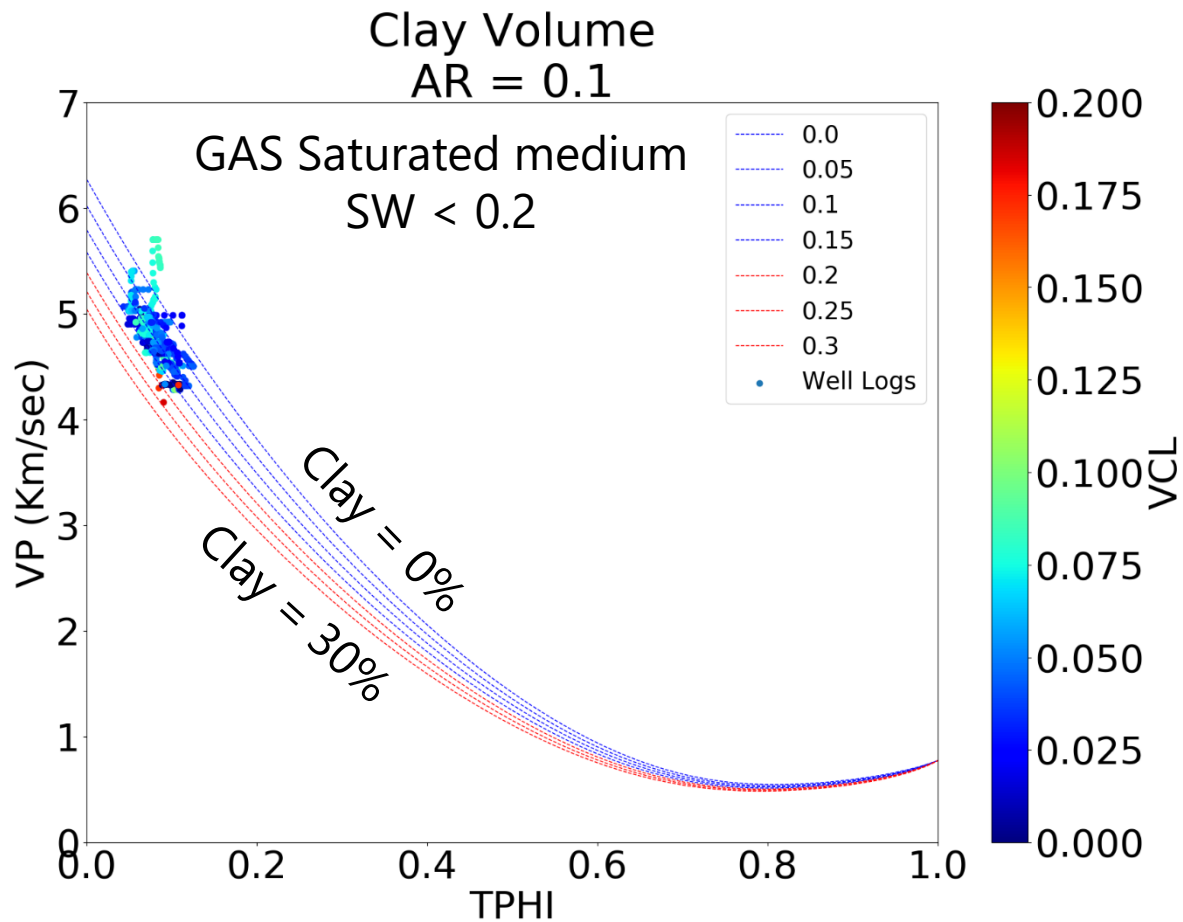


Clay Analysis

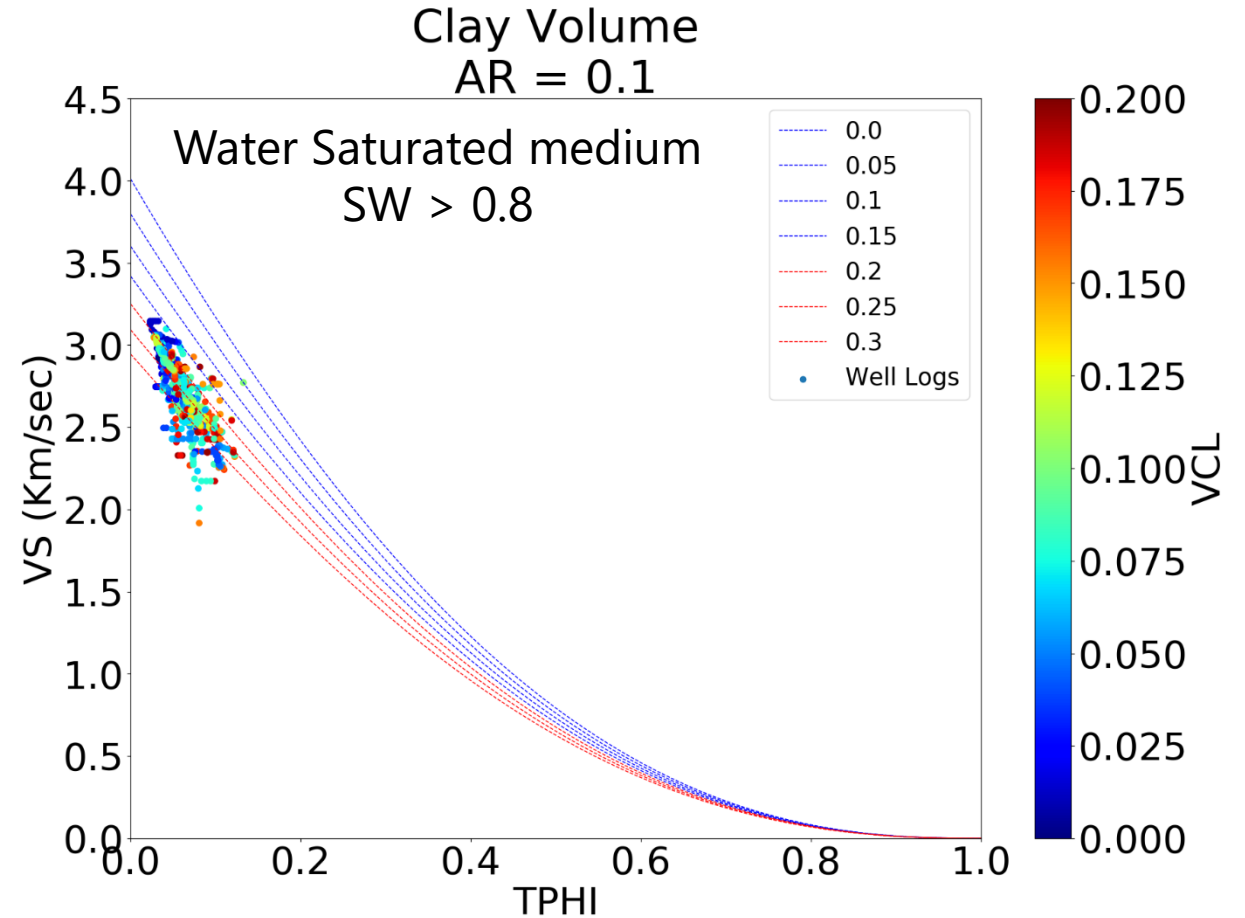
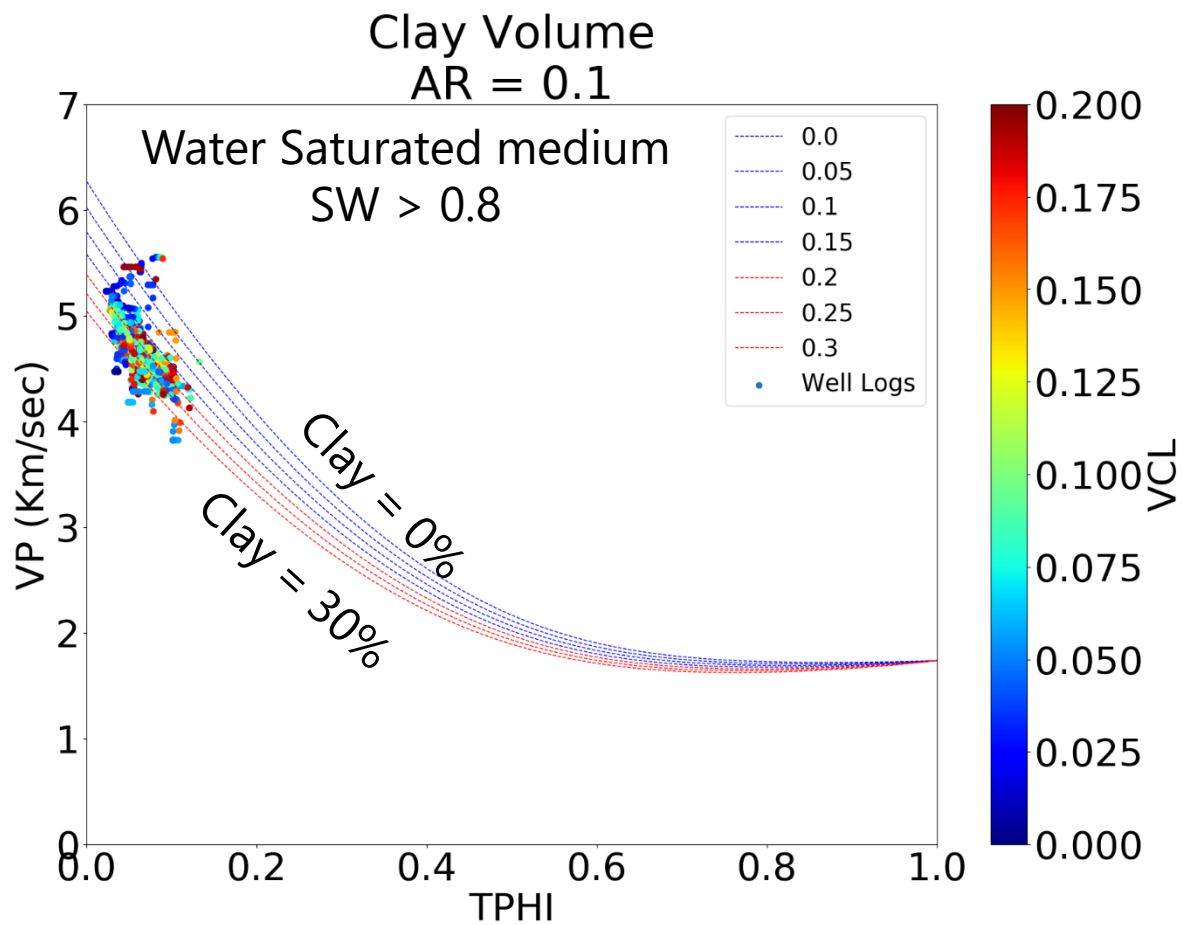
Water Saturated media
 $\alpha = 0.1$
Well Points = Gas saturated



Clay Analysis



Clay Analysis



SW x Velocities

